Experimental studies of RSAEs on Alcator C-Mod

E.M. Edlund[1], M. Porkolab[1], L. Lin[2], N. Tsujii[1], S.J. Wukitch[1]

[1]Massachusetts Institute of Technology, Cambridge, MA
[2]University of California Los Angeles, Los Angeles, CA

Energetic Particles Workshop, General Atomics
August 10, 2009

Presented by M. Porkolab

This work is supported by the US Department of Energy

Hollow current density profiles form as the Ohmic current diffuses toward the core

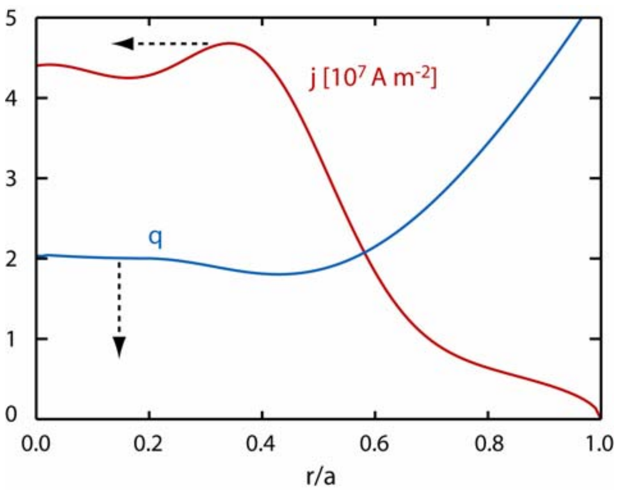

- Finite resistivity means that the current diffuses toward the core on a resistive time scale, in Alcator C-Mod this is

$$\tau_\eta \sim \frac{\mu_0 L^2}{\eta} \sim a^2 T_e^{3/2} \sim 200\ \mathrm{ms}\ \ (\mathrm{startup})$$

$$\sim 30\ \mathrm{ms}\ (\mathrm{sawteeth})$$

- ITER may achieve temperatures of 20+ keV during the current ramp

$$\tau_\eta \sim a^2 T_e^{3/2} \sim 300\ \mathrm{sec}\ \ (\mathrm{startup})$$

- Alfvén eigenmodes will likely be driven by beams, ICRH and α-particles

Reversed shear Alfvén eigenmodes (RSAEs) observed during the current ramp and sawteeth

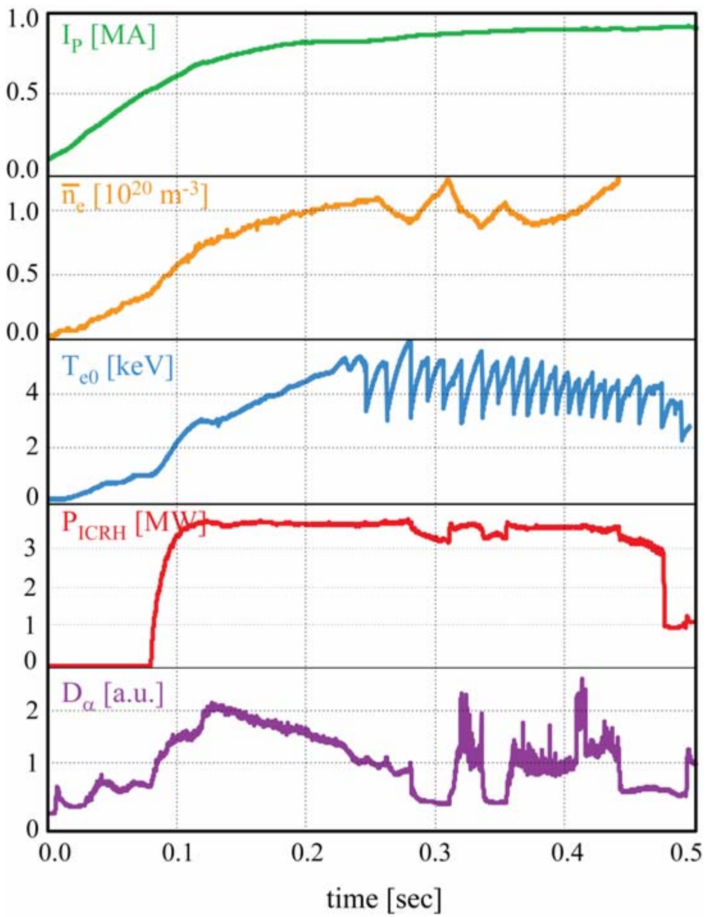

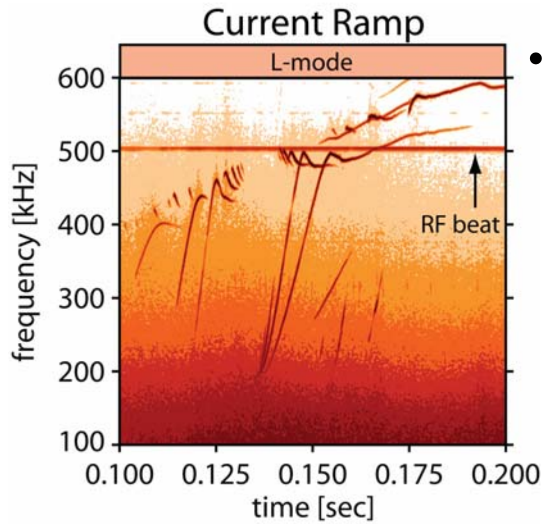

- RSAEs observed during the current ramp
  - MHD spectroscopy
  - No sawteeth
  - Good regime to study energetic particle transport?

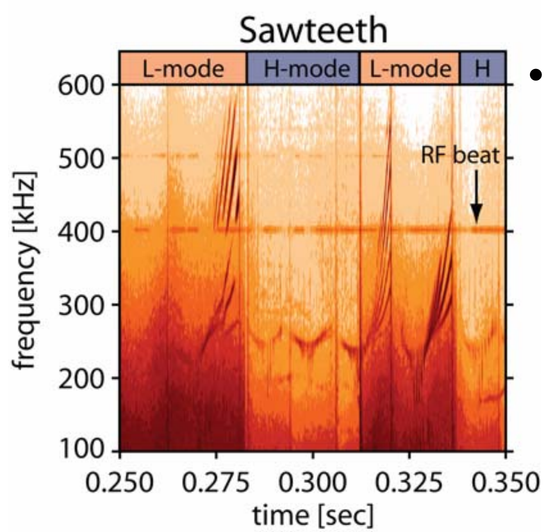

- RSAEs observed during sawteeth
  - Both L and H mode
  - Significant differences in RSAE excitation
  - T_e > 3 keV
  - n_{e0} < 1.5 x 10^{20} m^{-3}

The reversed shear Alfvén eigenmodes exhibit strong dependence on q_{min}

0-500 kHz ~200 kHz

$$\omega_{RSAE}^2 \approx \frac{V_A^2}{R_0^2}\left(\frac{m}{q_{\min}(t)} - n\right)^2 + \frac{2T_e}{M_i R_0^2}\left(1 + \frac{7}{4}\frac{T_i}{T_e}\right) - \frac{2}{M_i R_0^2} r \frac{d}{dr} T_e\left(1 + \frac{T_i}{T_e}\right) - \frac{\omega_{cH}\omega_{RSAE}}{m_{poloidal}} \frac{r}{n_e} \frac{d}{dr}\langle n_H \rangle$$

~100 kHz < 100 kHz ??

Breizman *et* al., PoP **12**, 112506 (2005) [kinetic effects]

Gorelenkov *et al.*, PPCF **48**, 1255 (2006) [MHD derivation]

The reversed shear Alfvén eigenmodes exhibit strong dependence on q_{min}

0-500 kHz ~200 kHz

$$\omega_{RSAE}^2 \approx \frac{V_A^2}{R_0^2}\left(\frac{m}{q_{\min}(t)} - n\right)^2 + \frac{2T_e}{M_i R_0^2}\left(1+\frac{7}{4}\frac{T_i}{T_e}\right) - \frac{2}{M_i R_0^2} r \frac{d}{dr} T_e \left(1+\frac{T_i}{T_e}\right) - \frac{\omega_{cH}\omega_{RSAE}}{m_{poloidal}} \frac{r}{n_e}\frac{d}{dr}\langle n_H \rangle$$

~100 kHz < 100 kHz ??

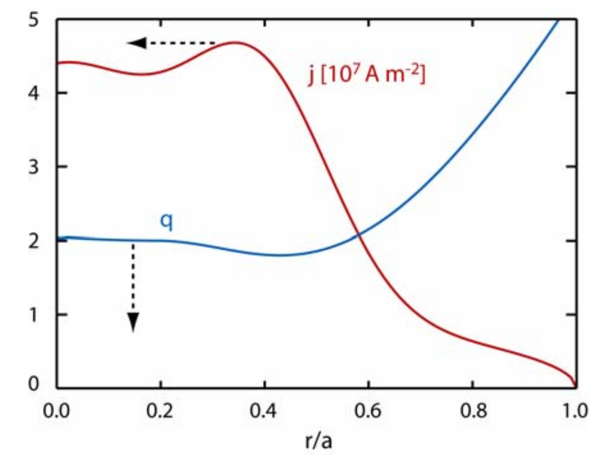

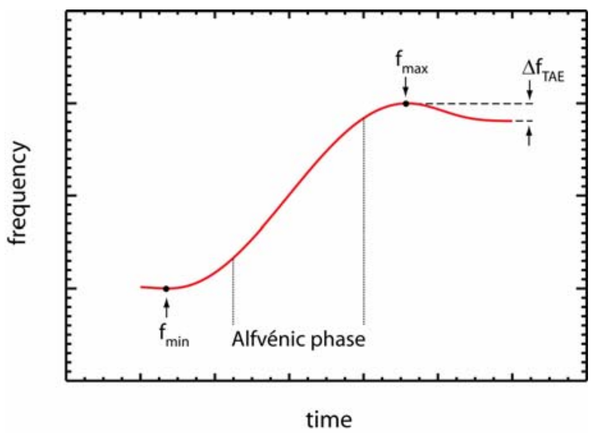

Breizman *et* al., PoP **12**, 112506 (2005) [kinetic effects]
Gorelenkov *et al.*, PPCF **48**, 1255 (2006) [MHD derivation]

Outline

- Phase contrast imaging and Mirnov coils
- RSAE minimum frequency scaling
- RSAE tunneling and edge penetration
- Observations during sawteeth

Phase contrast imaging and Mirnov coils are the primary tools for Alfvén wave studies in C-Mod

Phase Contrast Imaging (PCI)[1]

- PCI measures path-integrated electron density fluctuations

$$I_{PCI} \sim r_e \lambda_{laser} \int \tilde{n}_e \, dl$$

- 32 channel detector measures spatial structure between 0.6 m < R < 0.8 m
- Frequency Range
  2kHz < f < 5 MHz

Mirnov Coils

Coils at 6 toroidal locations are used to identify low-n modes

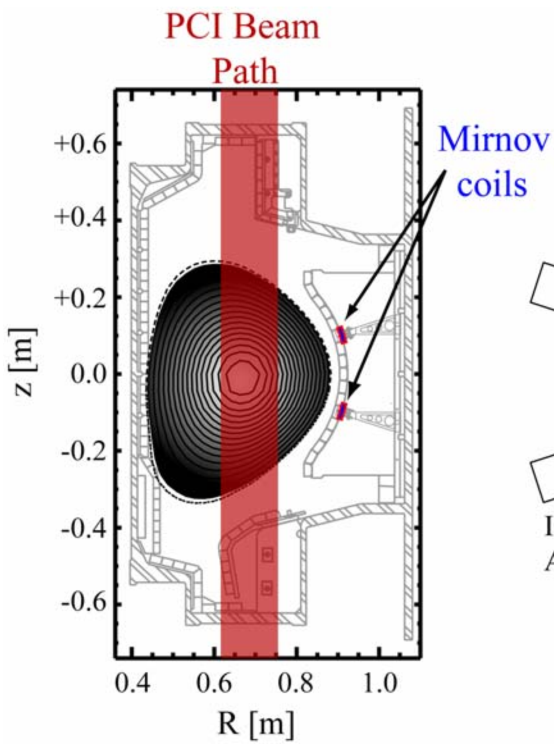

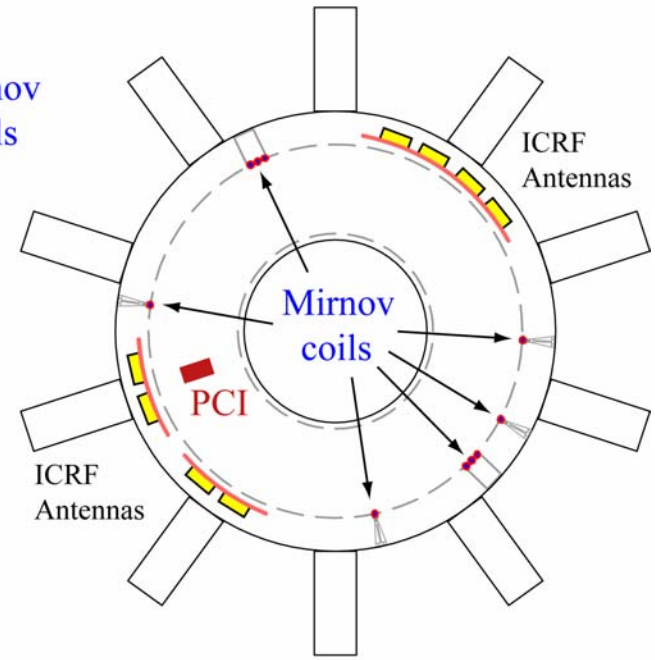

[1]M. Porkolab *et al.*, IEEE Trans. Plasma Sci. **34**, 229 (2006).

NOVA[1] results are compared to experiment with a synthetic PCI analysis[2]

(3 clicks)

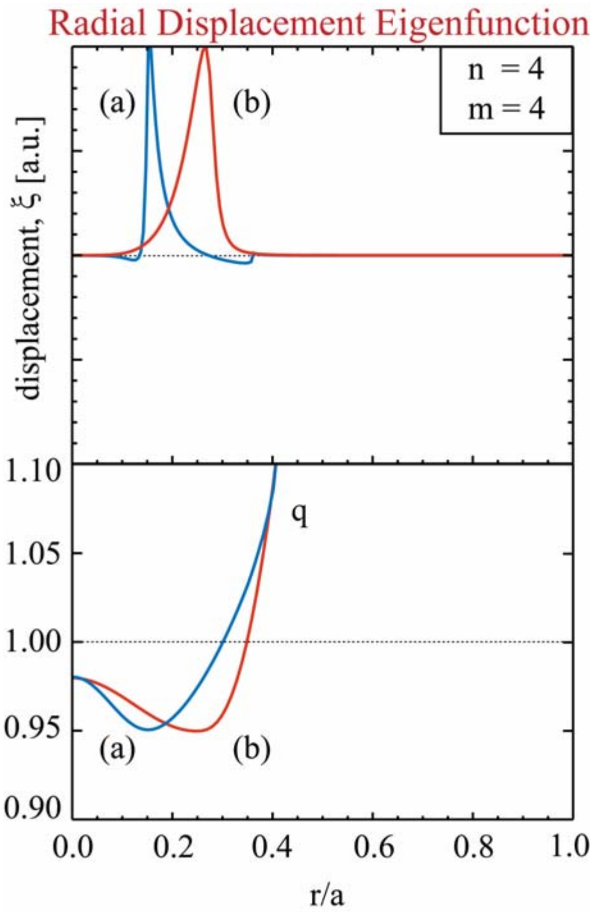

[1]Cheng and Chance, J. Comput. Phys. **71**, 124 (1987).

[2]Synthetic PCI developed in collaboration with Gerrit Kramer.

NOVA[1] results are compared to experiment with a synthetic PCI analysis[2]

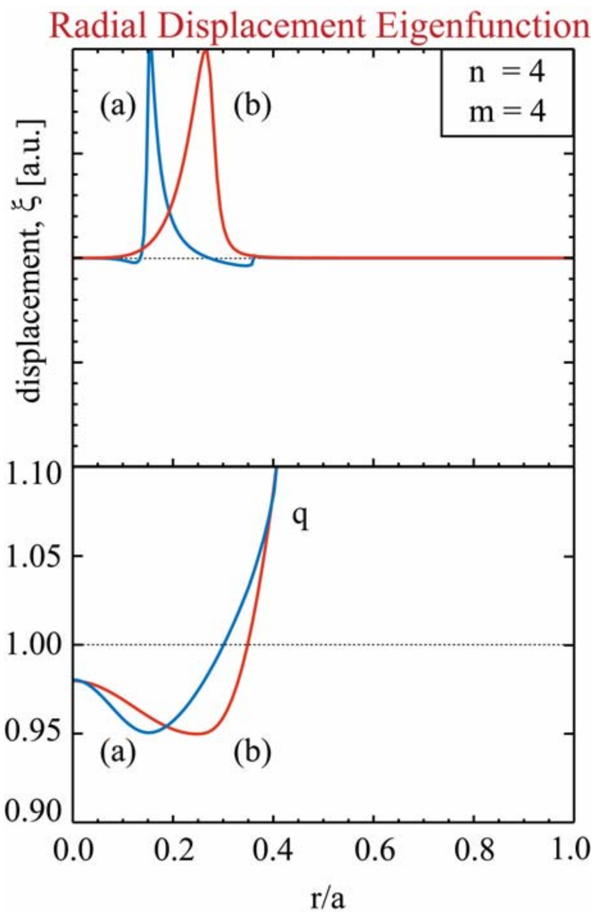

$$\xi \Rightarrow \tilde{n}_e$$

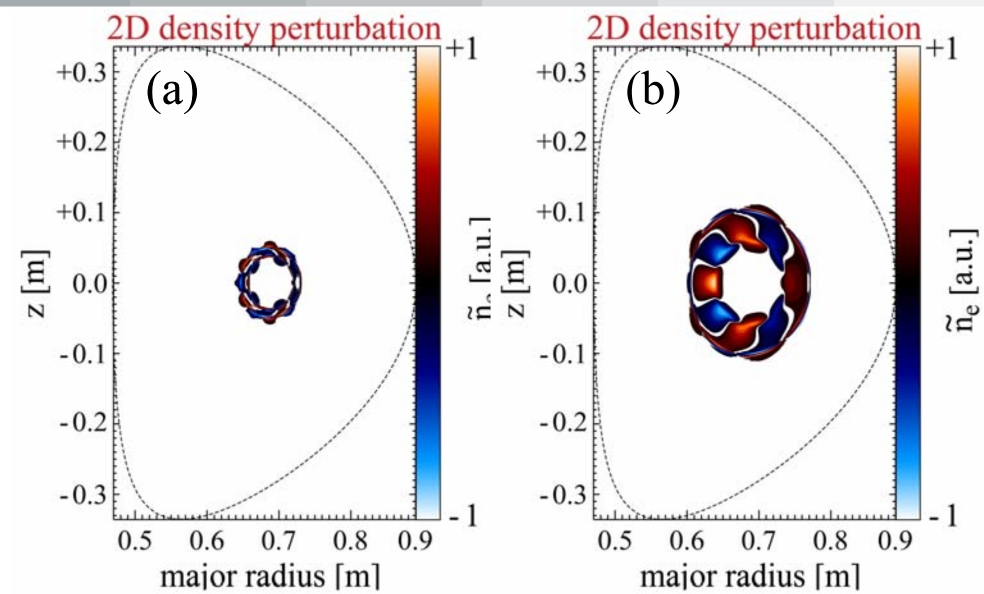

[1]Cheng and Chance, J. Comput. Phys. **71**, 124 (1987).

[2]Synthetic PCI developed in collaboration with Gerrit Kramer.

NOVA[1] results are compared to experiment with a synthetic PCI analysis[2]

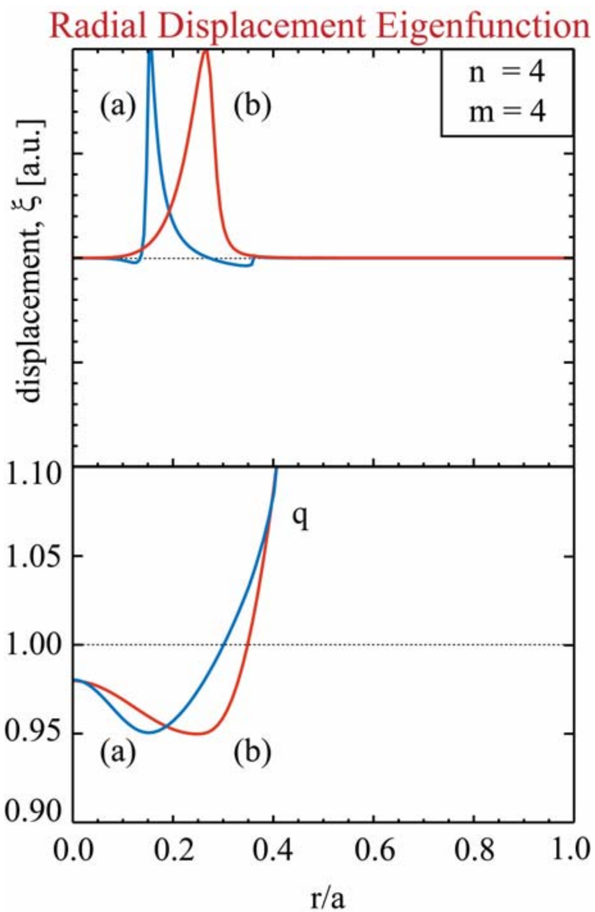

$$\xi \Rightarrow \tilde{n}_e$$

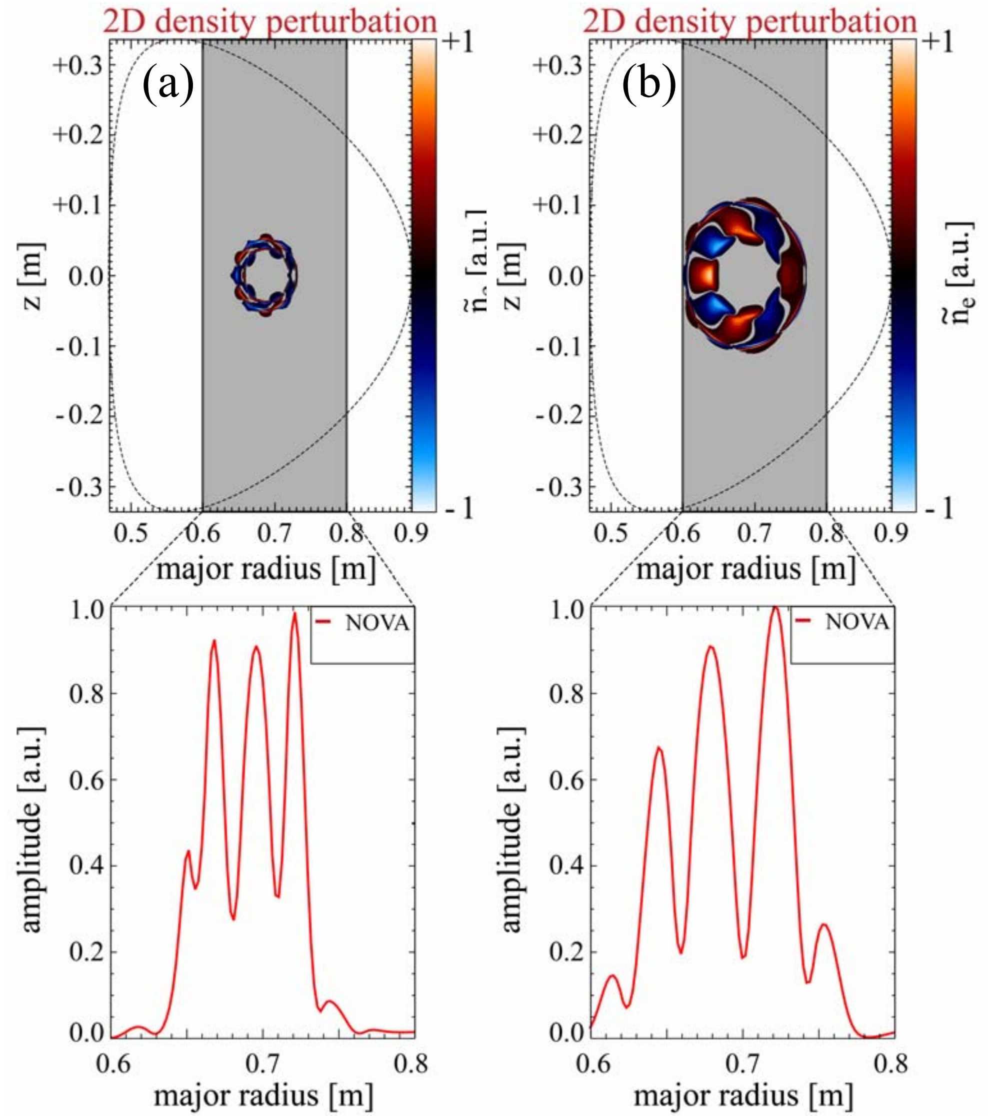

[1]Cheng and Chance, J. Comput. Phys. **71**, 124 (1987).

[2]Synthetic PCI developed in collaboration with Gerrit Kramer.

NOVA[1] results are compared to experiment with a synthetic PCI analysis[2]

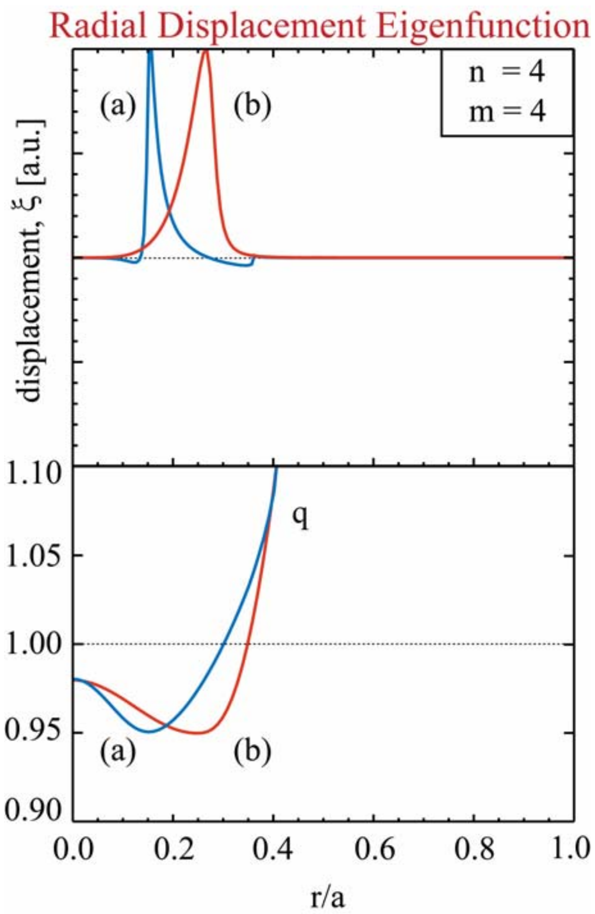

$$\xi \Rightarrow \tilde{n}_e$$

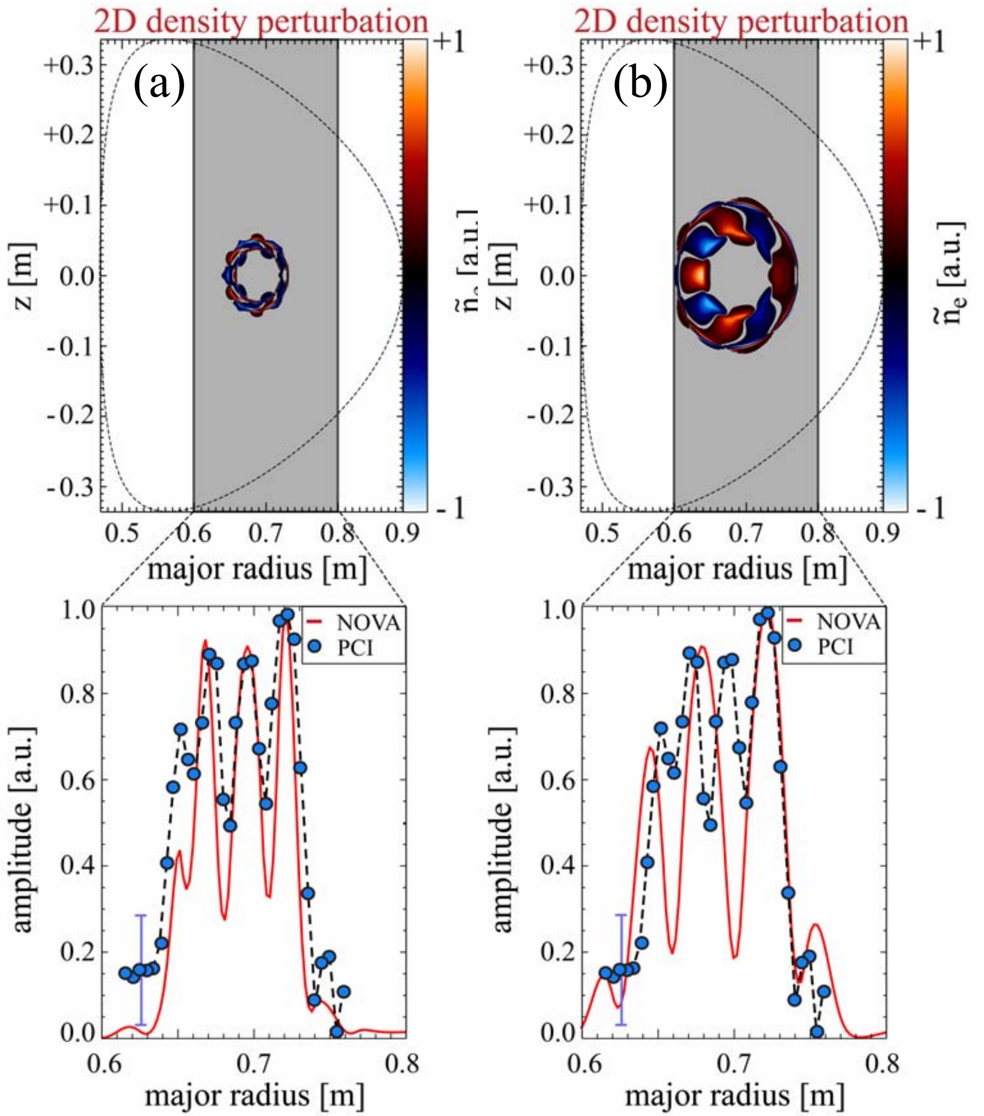

[1]Cheng and Chance, J. Comput. Phys. **71**, 124 (1987).

[2]Synthetic PCI developed in collaboration with Gerrit Kramer.

Minimum Frequency Scaling

(2 clicks)

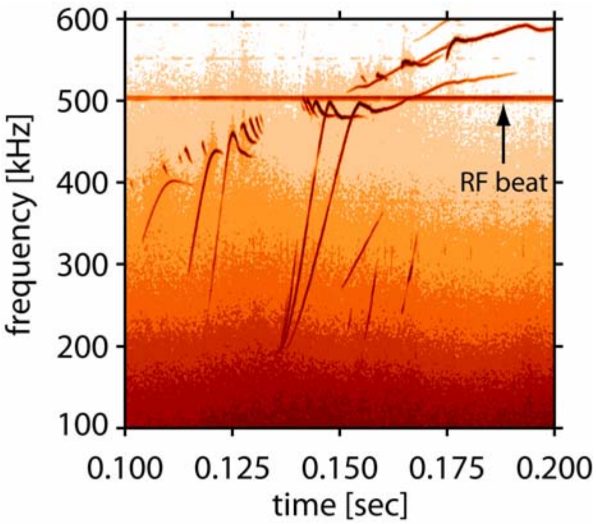

Minimum frequency expected to scale with T_e

$$f_{min}[\text{kHz}] \approx 100 T_e^{1/2} \sqrt{0.75\gamma + 0.15 \frac{a}{L_T}}$$

NOVA scaling

$$f_{min}[\text{kHz}] \approx 70 T_e^{1/2} \sqrt{\left(1 + \frac{7}{4}\frac{T_i}{T_e}\right) + 0.3\left(1 + \frac{T_i}{T_e}\right)\frac{a}{L_T}}$$

Breizman *et al.* scaling

Agree within 10% when $T_i/T_e = 0.8$

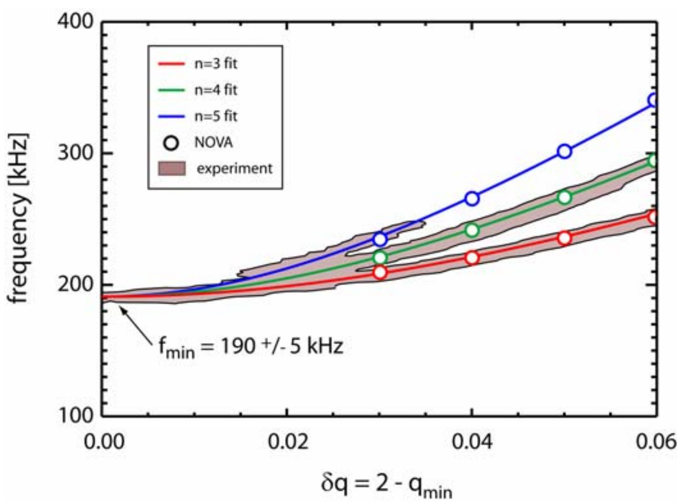

Minimum Frequency Scaling

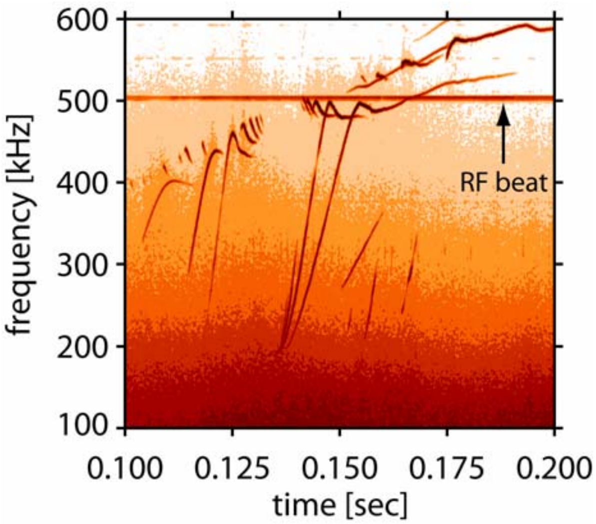

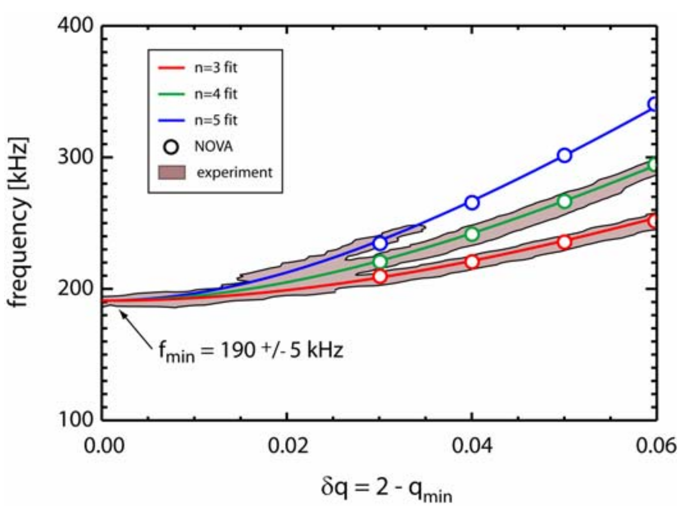

Minimum frequency expected to scale with T_e

$$f_{\min}[\text{kHz}] \approx 100 T_e^{1/2} \sqrt{0.75\gamma + 0.15\frac{a}{L_T}}$$

NOVA scaling

$$f_{\min}[\text{kHz}] \approx 70 T_e^{1/2} \sqrt{\left(1 + \frac{7}{4}\frac{T_i}{T_e}\right) + 0.3\left(1 + \frac{T_i}{T_e}\right)\frac{a}{L_T}}$$

Breizman *et al.* scaling

Agree within 10% when $T_i/T_e = 0.8$

MHD equation of state

$$\frac{\mathrm{d}}{\mathrm{d}t}\left(\frac{p}{\rho^{\gamma}}\right) = 0$$

Minimum Frequency Scaling

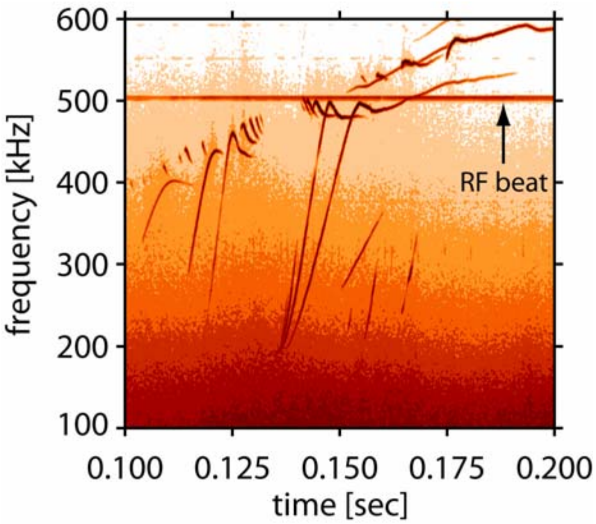

Minimum frequency expected to scale with T_e

$$f_{\min}[\text{kHz}] \approx 100 T_e^{1/2} \sqrt{0.75\gamma + 0.15\frac{a}{L_T}}$$

NOVA scaling

$$f_{\min}[\text{kHz}] \approx 70 T_e^{1/2} \sqrt{\left(1+\frac{7}{4}\frac{T_i}{T_e}\right) + 0.3\left(1+\frac{T_i}{T_e}\right)\frac{a}{L_T}}$$

Breizman *et al.* scaling

Agree within 10% when $T_i/T_e = 0.8$

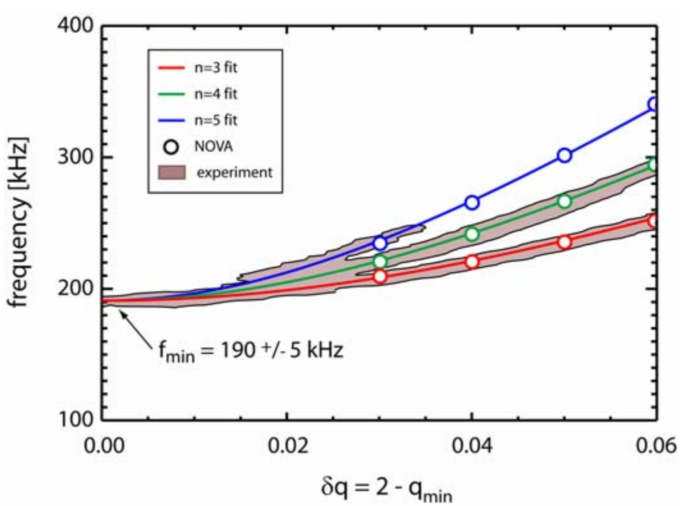

MHD equation of state

$$\frac{d}{dt}\left(\frac{p}{\rho^{\gamma}}\right) = 0$$

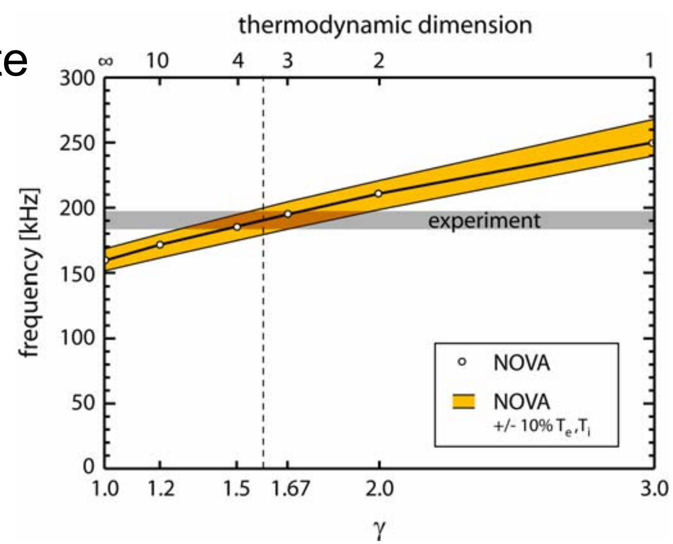

Minimum Frequency Scaling

(2 clicks)

PCI measurements support
$1.25 \leq \gamma \leq 1.55$

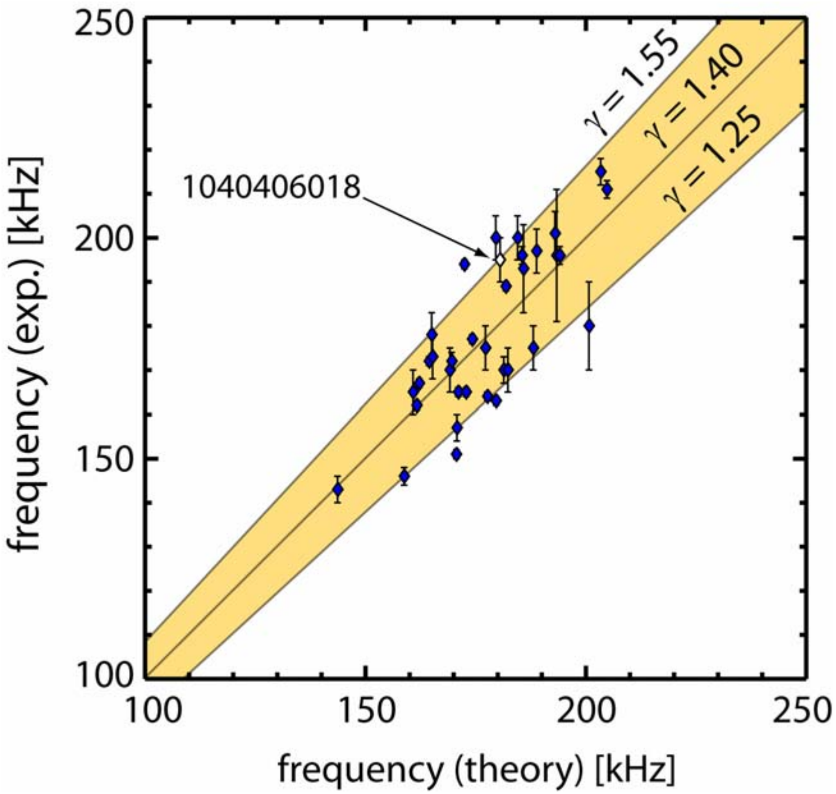

[1]McKee and Zweibel, Astro. J. **440**, 686 (1995).

Minimum Frequency Scaling

PCI measurements support
$1.25 \leq \gamma \leq 1.55$

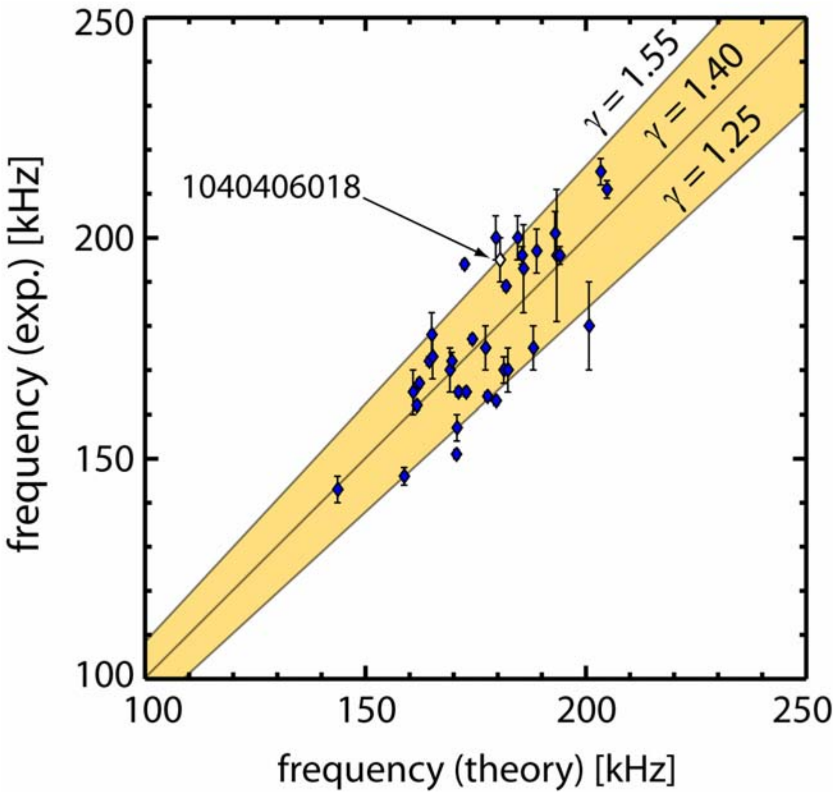

For shear Alfvén waves[1] (no geometric effects)

$$v_1 \approx \frac{B_1}{\sqrt{\mu_0 \rho}}$$

$$U = \tfrac{1}{2\mu_0} B_1^2 + \tfrac{1}{2} \rho v_1^2 = \tfrac{1}{\mu_0} B_1^2$$

$$\mathbf{P} = \tfrac{1}{2\mu_0} B_1^2 \mathbf{I} - \tfrac{1}{2\mu_0} \mathbf{B}_1 \mathbf{B}_1 + \rho \mathbf{v}_1 \mathbf{v}_1 = \tfrac{1}{2\mu_0} B_1^2 \mathbf{I}$$

$$P = (\gamma - 1) U \quad \rightarrow \quad \gamma = \tfrac{3}{2}$$

---

[1] McKee and Zweibel, Astro. J. **440**, 686 (1995).

Minimum Frequency Scaling

PCI measurements support
$1.25 \leq \gamma \leq 1.55$

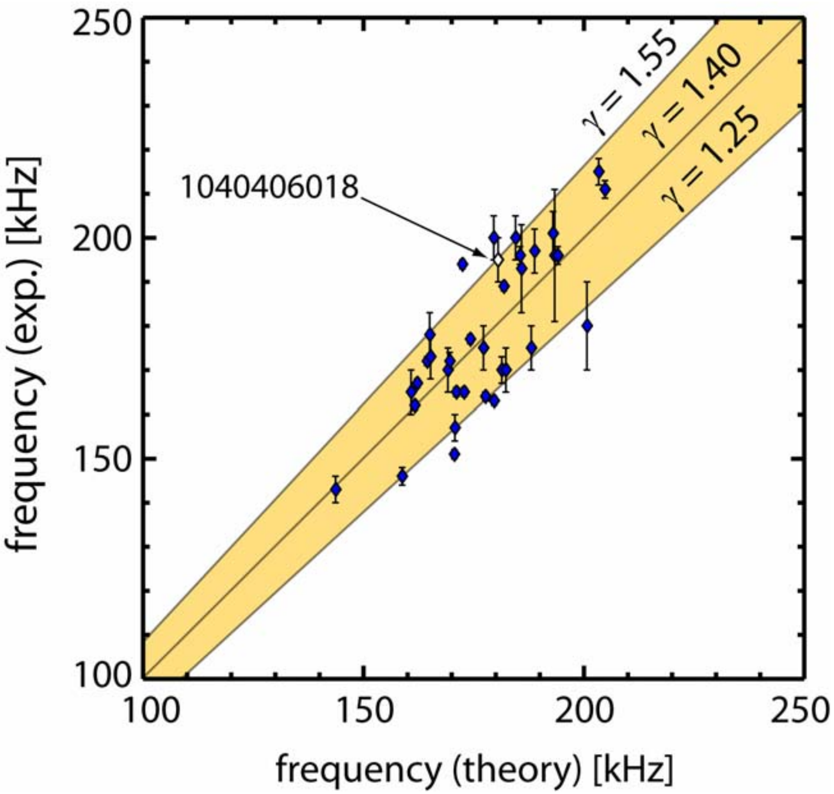

For shear Alfvén waves[1] (no geometric effects) $v_1 \approx \frac{B_1}{\sqrt{\mu_0 \rho}}$

$$U = \tfrac{1}{2\mu_0} B_1^2 + \tfrac{1}{2}\rho v_1^2$$
$$= \tfrac{1}{\mu_0} B_1^2$$

$$\mathbf{P} = \tfrac{1}{2\mu_0} B_1^2 \mathbf{I} - \tfrac{1}{2\mu_0} \mathbf{B}_1 \mathbf{B}_1 + \rho \mathbf{v}_1 \mathbf{v}_1$$
$$= \tfrac{1}{2\mu_0} B_1^2 \mathbf{I}$$

$$P = (\gamma - 1)U \quad \rightarrow \quad \gamma = \tfrac{3}{2}$$

Kinetic electrons: $\frac{v_{th,e}}{v_A} \sim 2$

[1]McKee and Zweibel, Astro. J. **440**, 686 (1995).

Core localized RSAEs must "tunnel" through the Alfvén continuum to reach the Mirnov coils

(5 clicks)

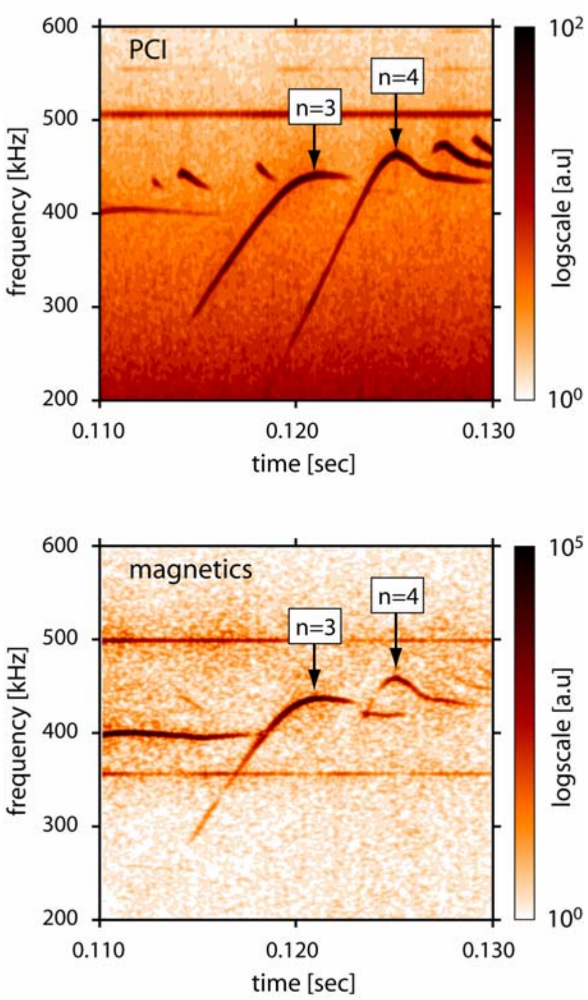

Core localized RSAEs must “tunnel” through the Alfvén continuum to reach the Mirnov coils

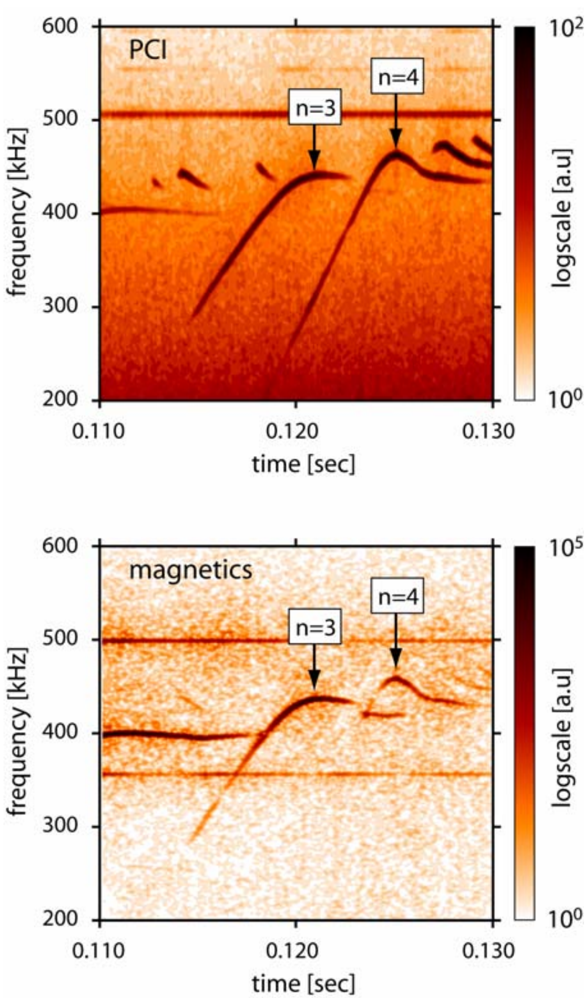

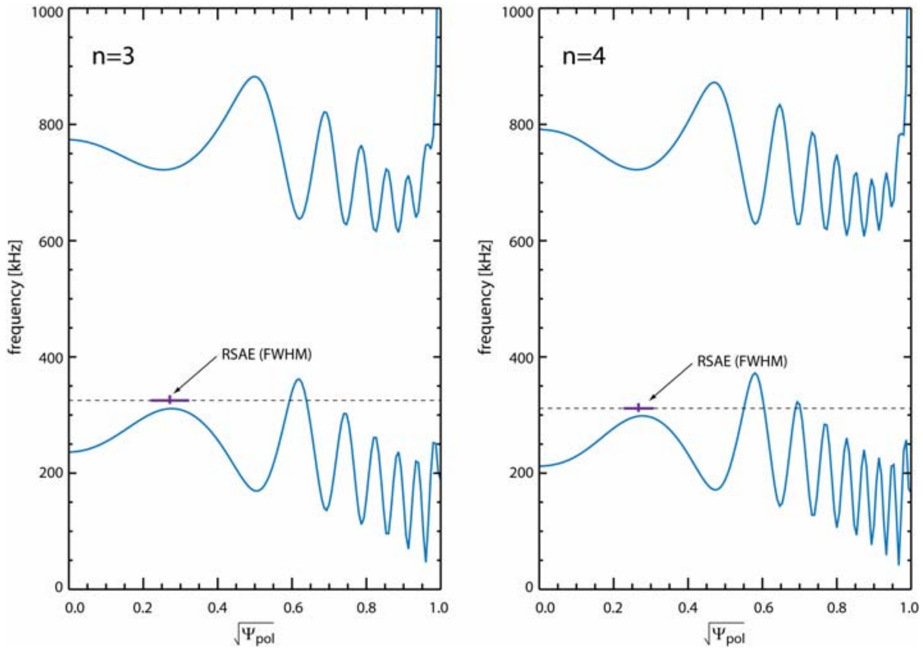

Core localized RSAEs must “tunnel” through the Alfvén continuum to reach the Mirnov coils

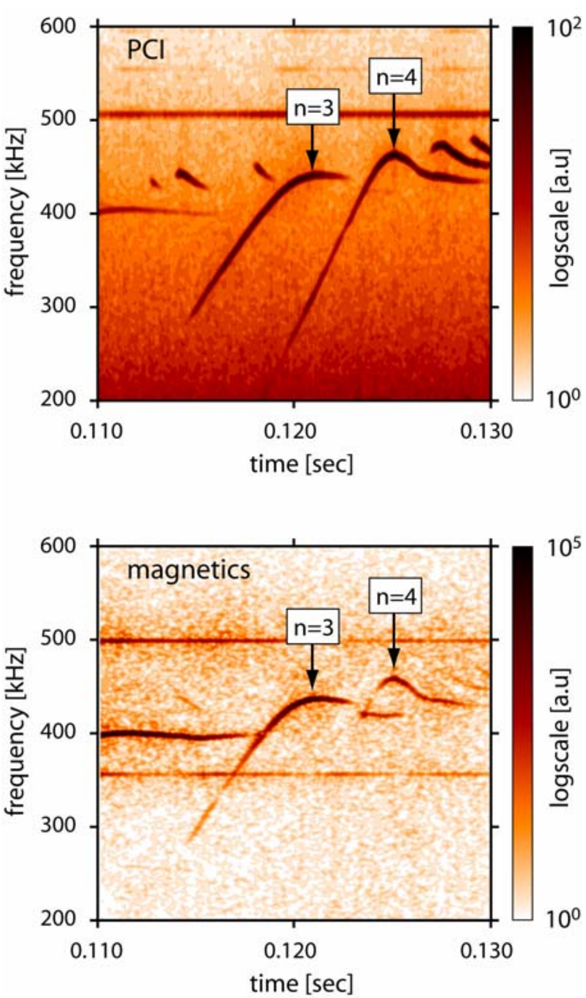

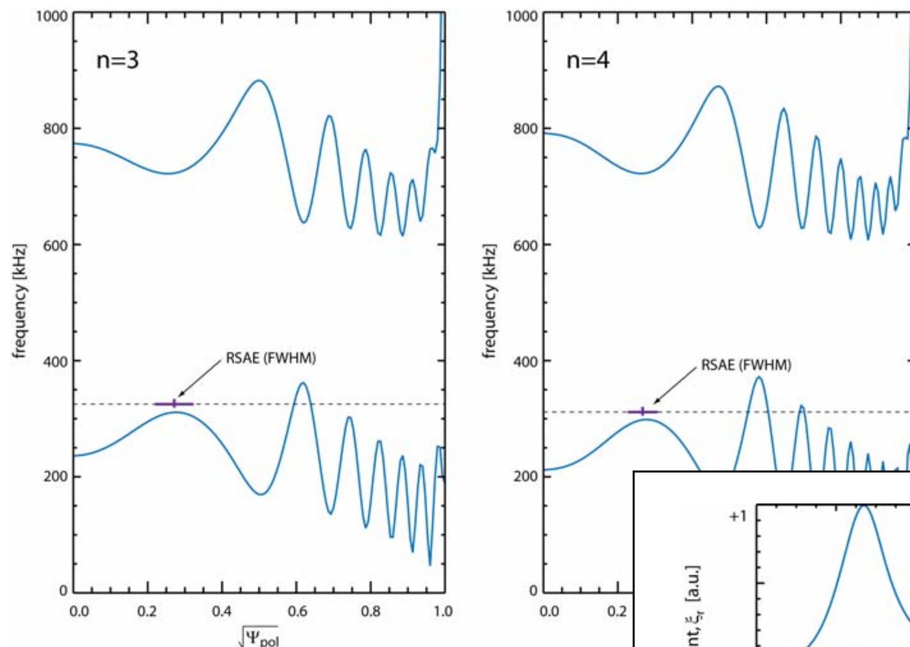

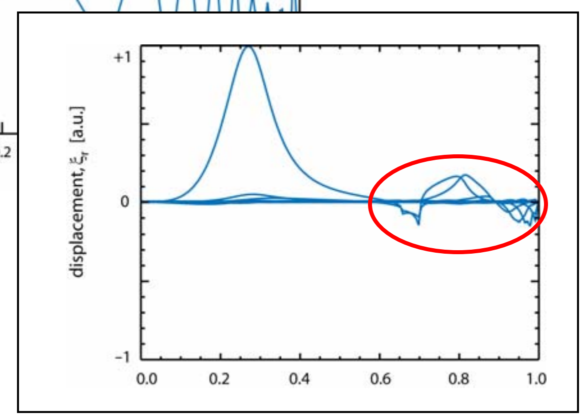

Q: How does tunneling affect the edge amplitude?

Core localized RSAEs must "tunnel" through the Alfvén continuum to reach the Mirnov coils

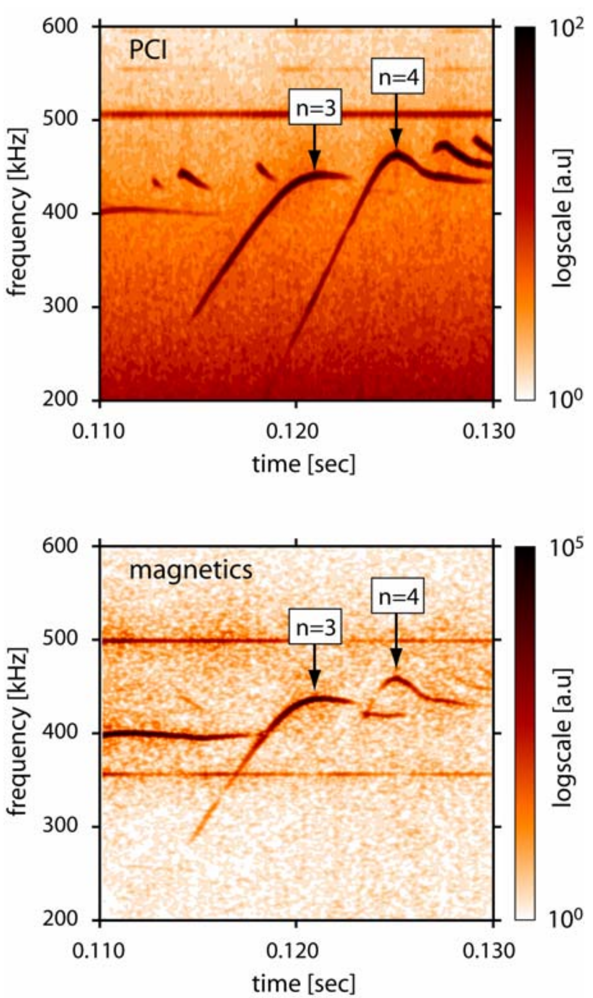

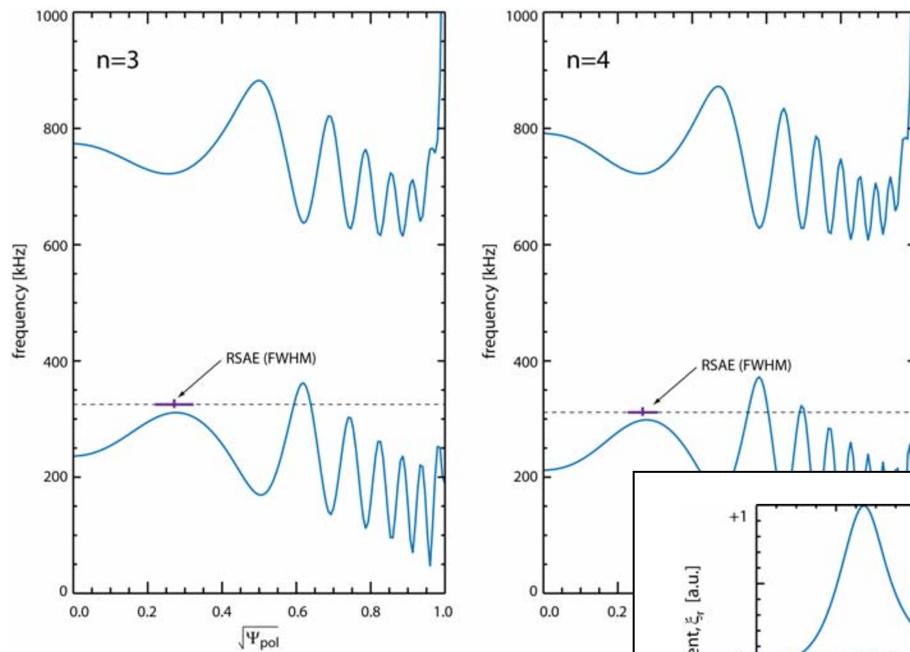

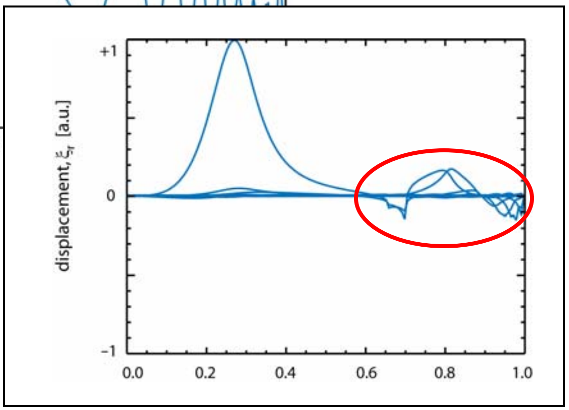

Q: How does tunneling affect the edge amplitude?

A: #1 Compare PCI and magnetics

#2 Simulate the effect with NOVA

Core localized RSAEs must "tunnel" through the Alfvén continuum to reach the Mirnov coils

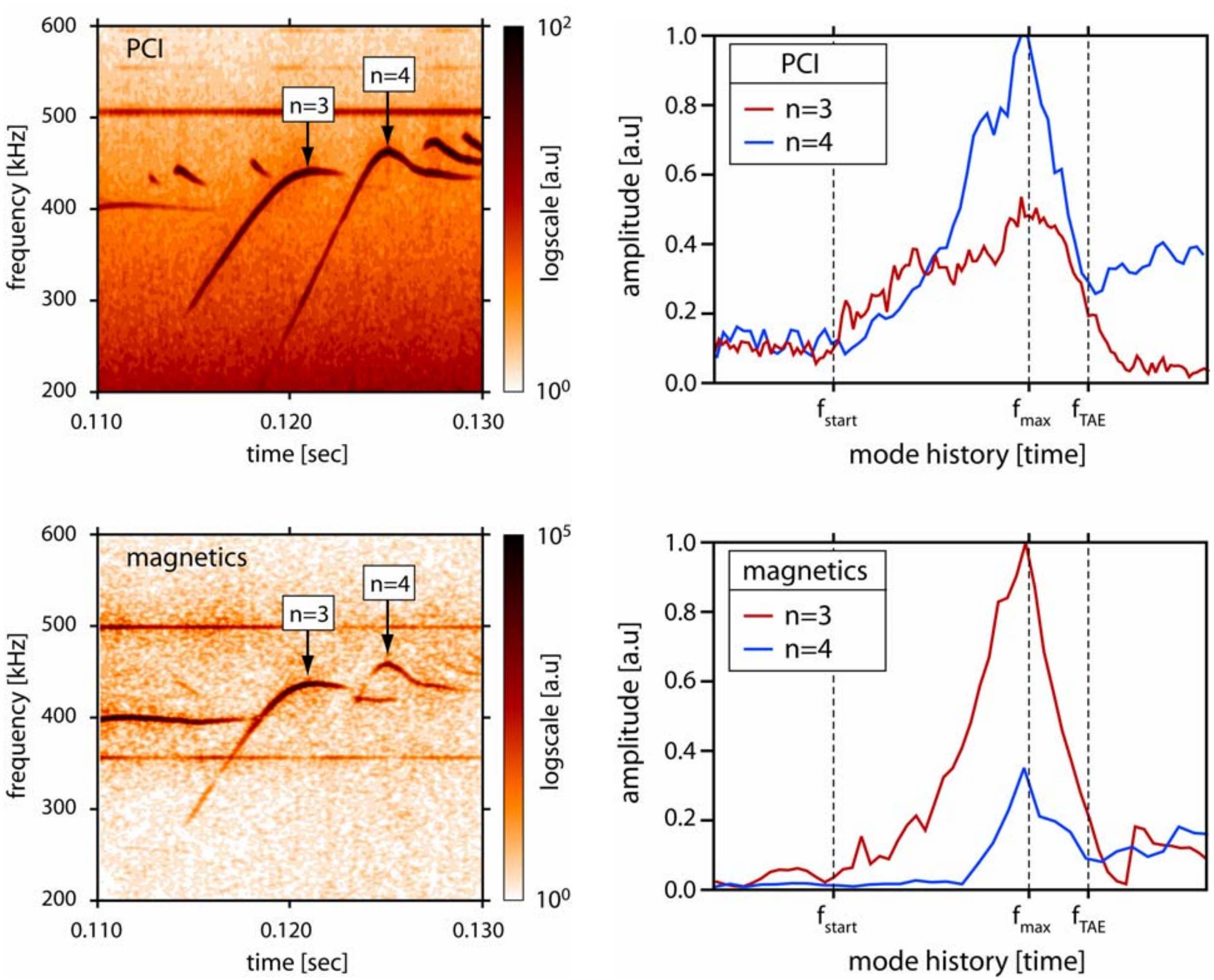

Core localized RSAEs must "tunnel" through the Alfvén continuum to reach the Mirnov coils

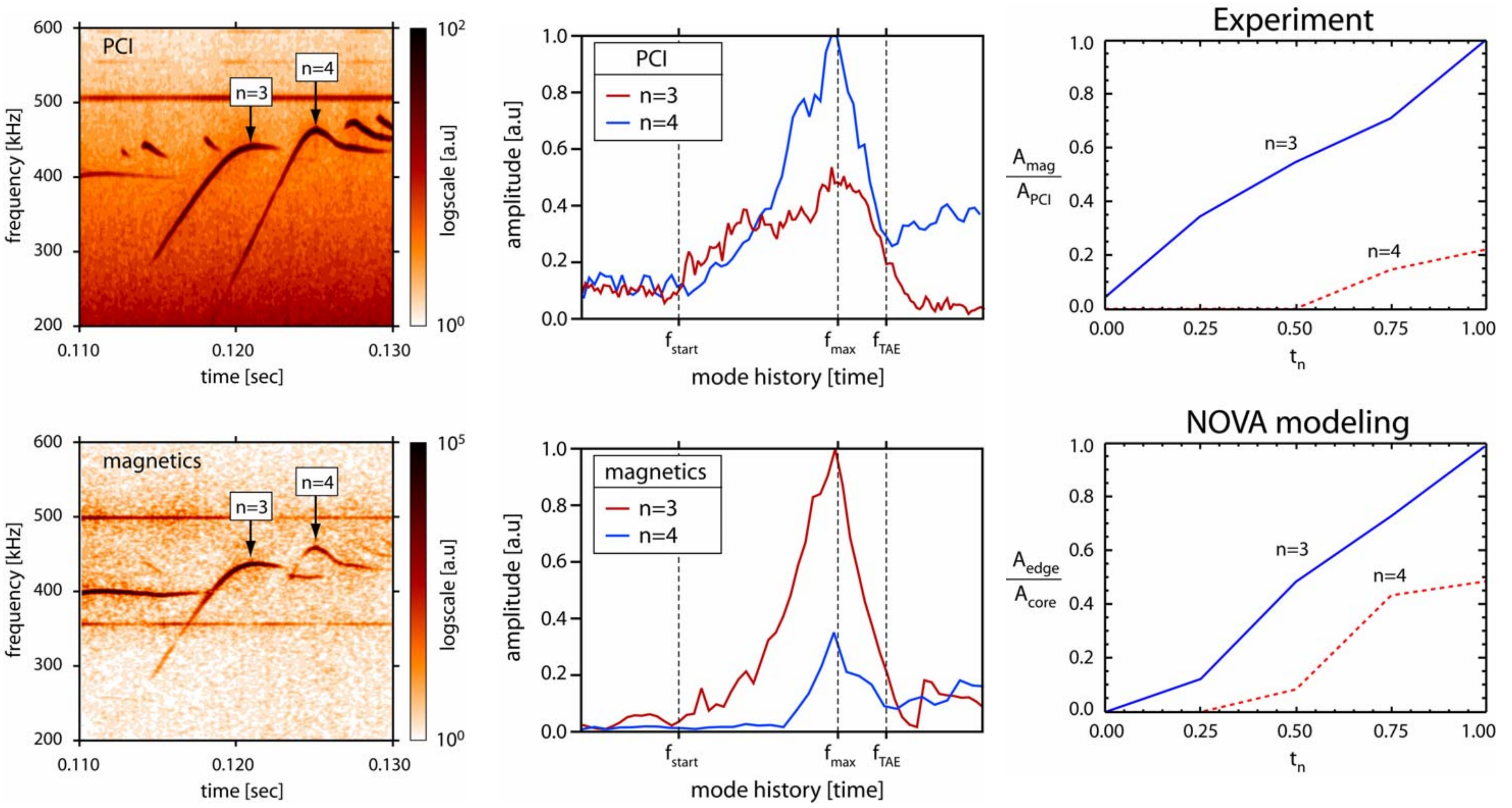

Future experiments may be able to test this effect over a wider range of conditions

(2 clicks)

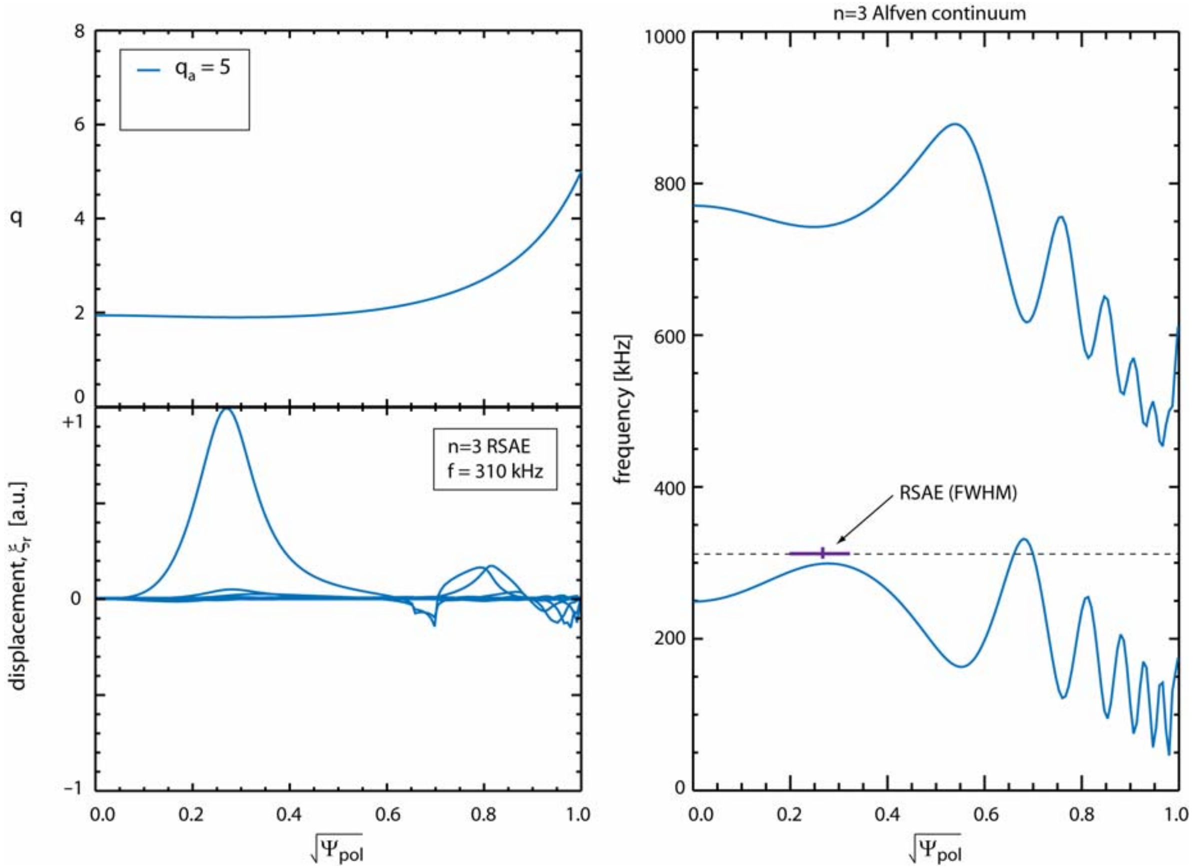

Alfvén continuum should vary strongly with

- plasma current
- edge density
- plasma shaping?

Future experiments may be able to test this effect over a wider range of conditions

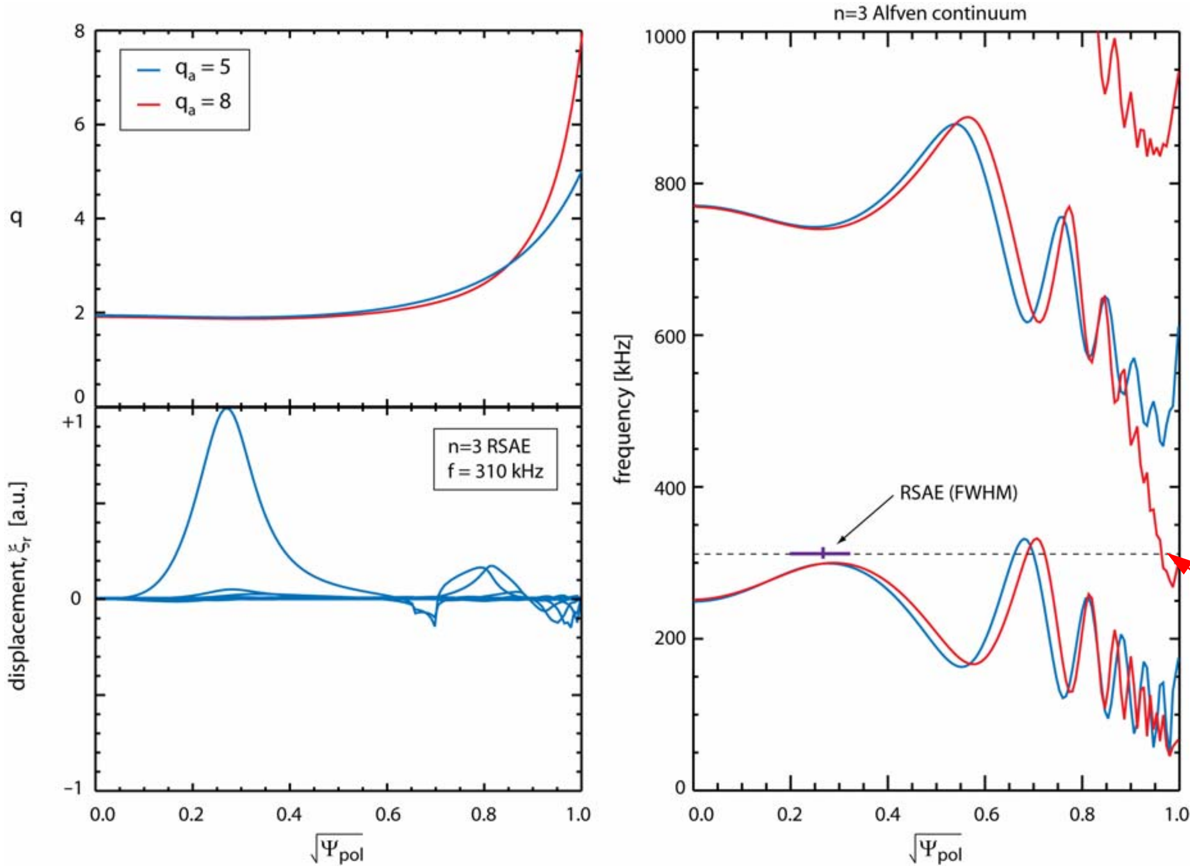

Alfvén continuum should vary strongly with

- plasma current
- edge density
- plasma shaping?

An additional barrier is presented to the eigenmodes in the case with larger edge q

Future experiments may be able to test this effect over a wider range of conditions

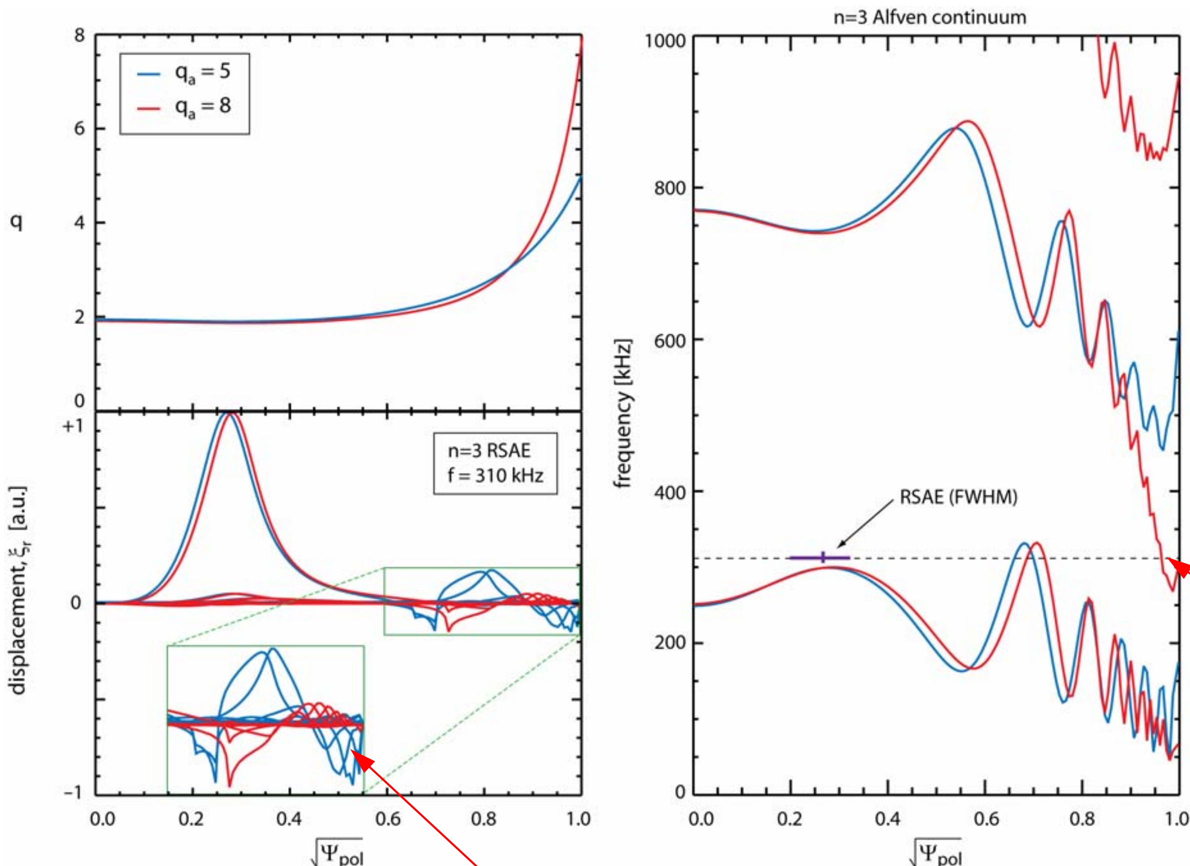

Alfvén continuum should vary strongly with

- plasma current
- edge density
- plasma shaping?

An additional barrier is presented to the eigenmodes in the case with larger edge q

Edge amplitude decreases

RSAEs excited during sawteeth show both up-chirping and down-chirping patterns

(2 clicks)

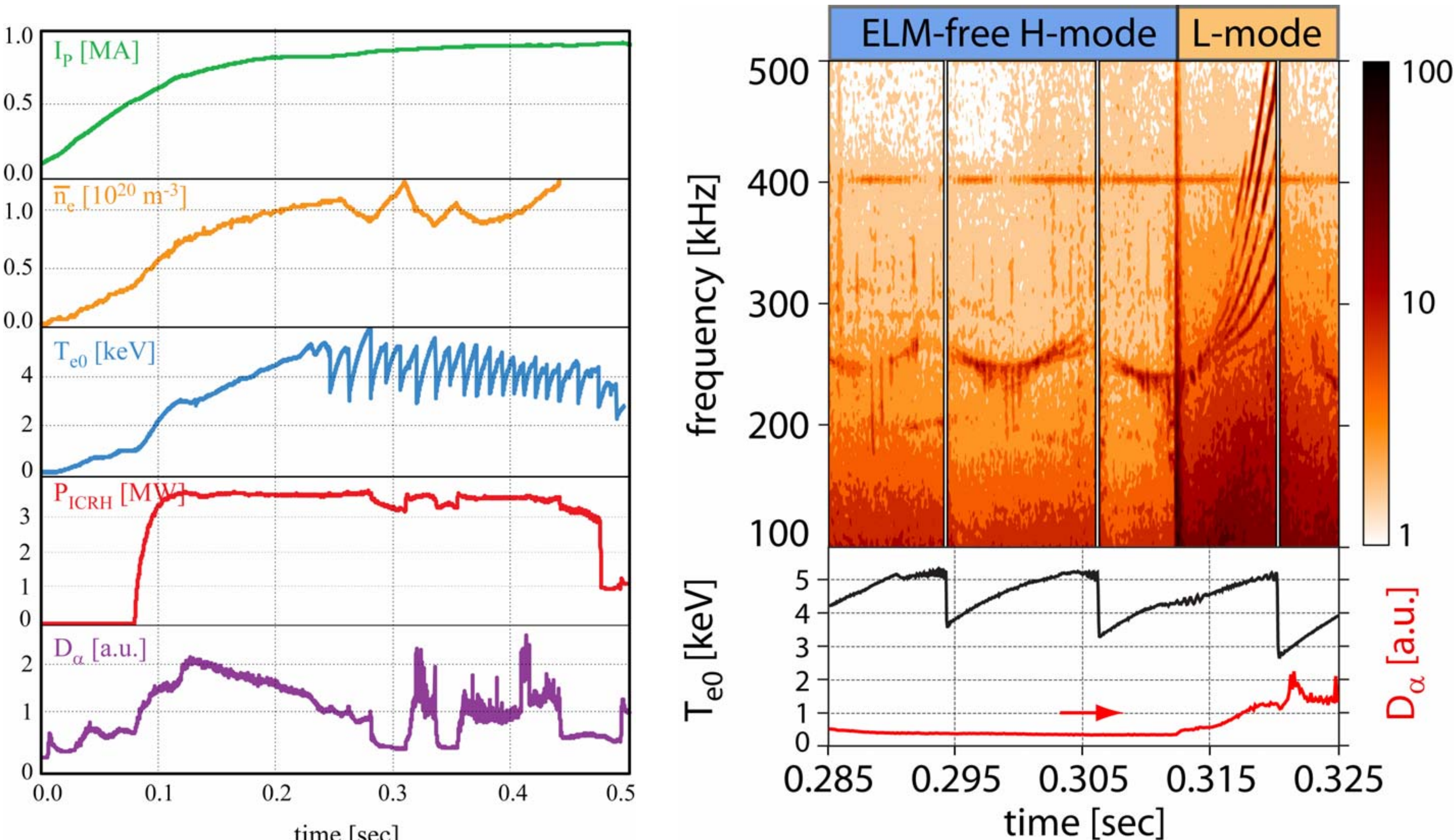

RSAEs excited during sawteeth show both up-chirping and down-chirping patterns

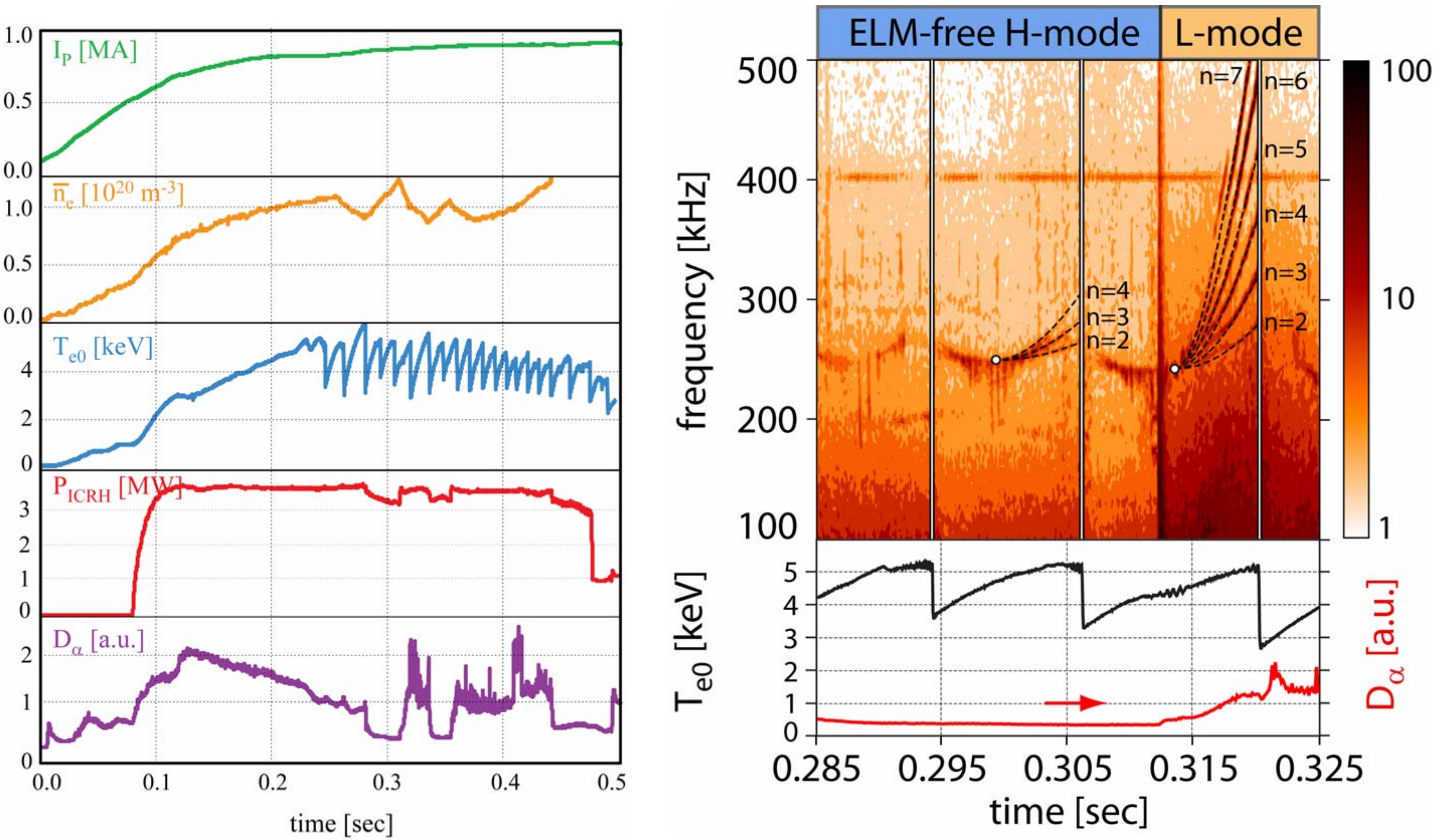

RSAEs excited during sawteeth show both up-chirping and down-chirping patterns

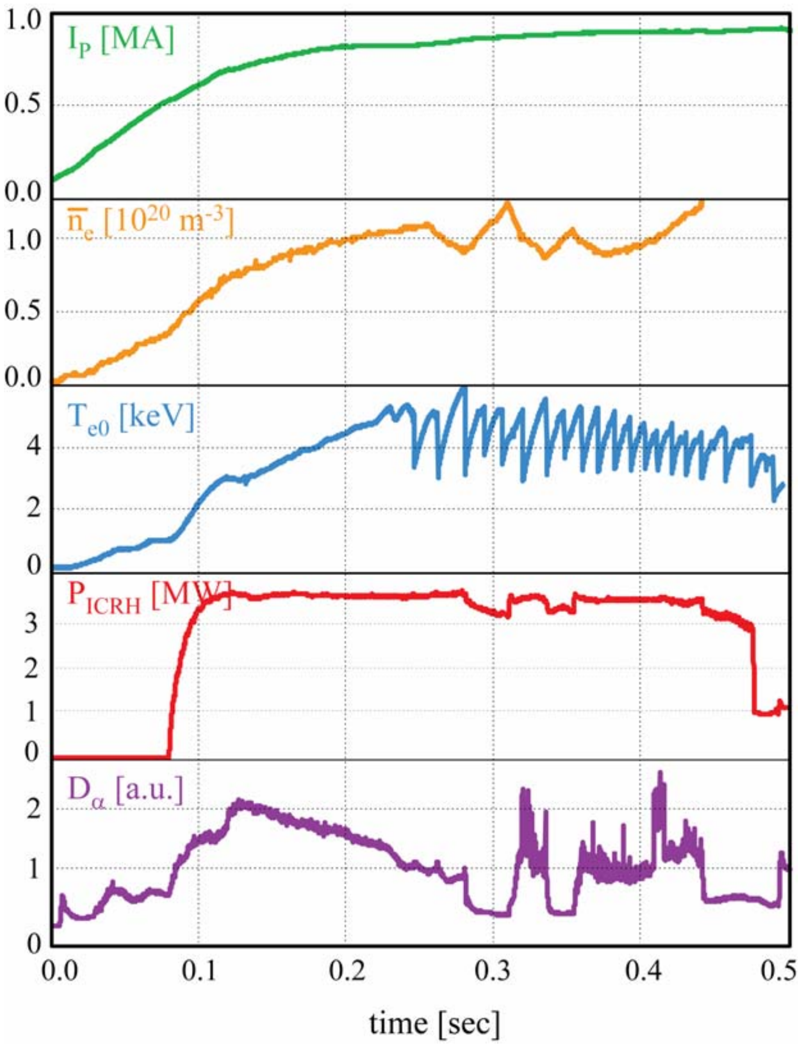

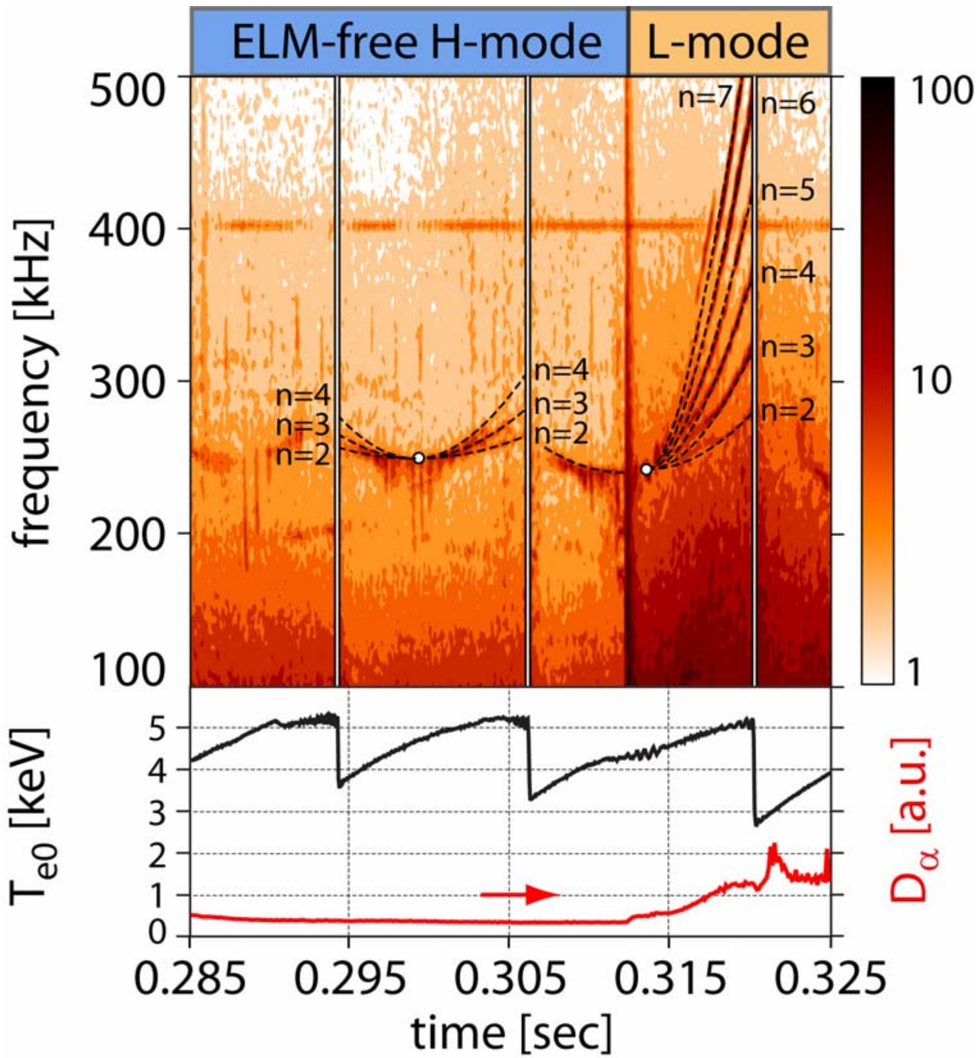

q=1 RSAEs are observed with PCI and magnetics

- RSAEs during sawteeth have been observed with PCI and Mirnov Coils
- PCI spectra are used to infer mode numbers from $$f_n^2 = f_0^2 + f_A^2\left(\frac{m}{q_{\min}} - n\right)^2$$
- Mirnov coils directly measure the toroidal phase $$m = n \quad \text{near} \quad q = 1$$

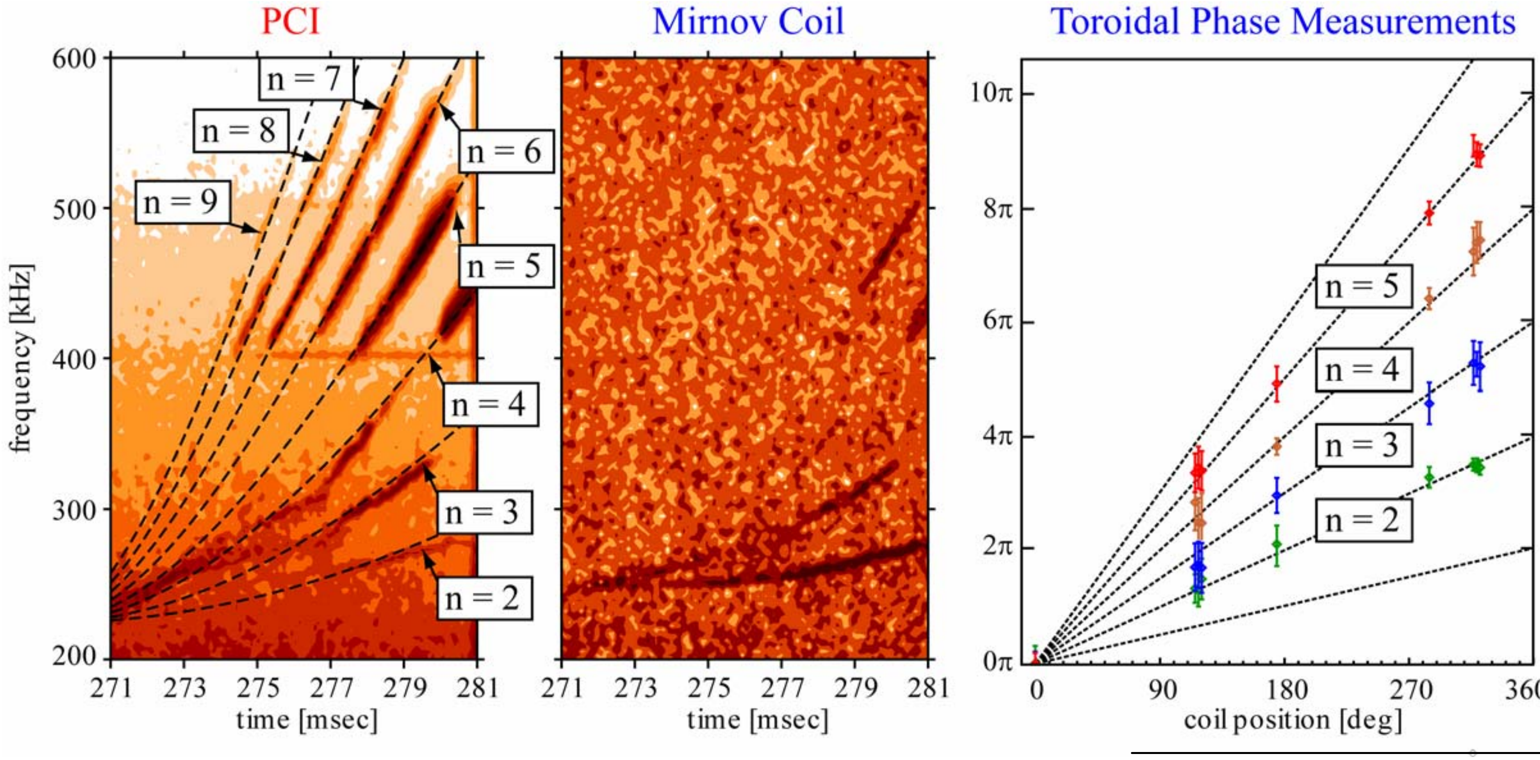

Edlund *et al.*, PoP **16**, 056106 (2009).

Down-chirping RSAEs constrain the post-crash q profile

- Faint down chirping RSAEs are frequently observed during sawteeth
- Strong down-chirping RSAEs followed a large sawtooth crash

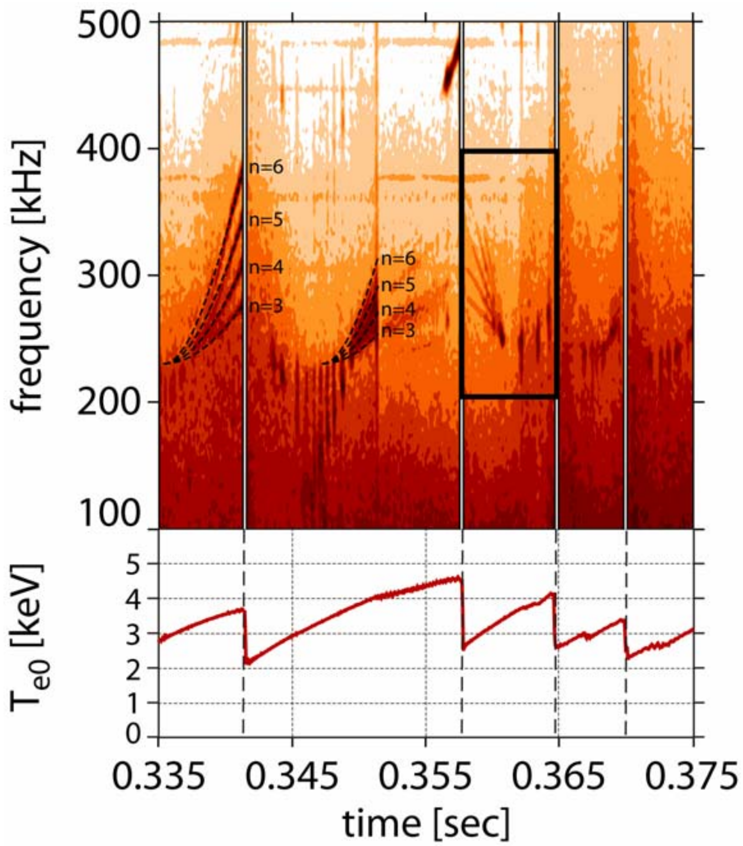

Down-chirping RSAEs constrain the post-crash q profile

- Faint down chirping RSAEs are frequently observed during sawteeth
- Strong down-chirping RSAEs followed a large sawtooth crash
- Mode numbers and spatial structure can be clearly identified
- What q profile following the sawtooth crash can result in down-chirping RSAEs?

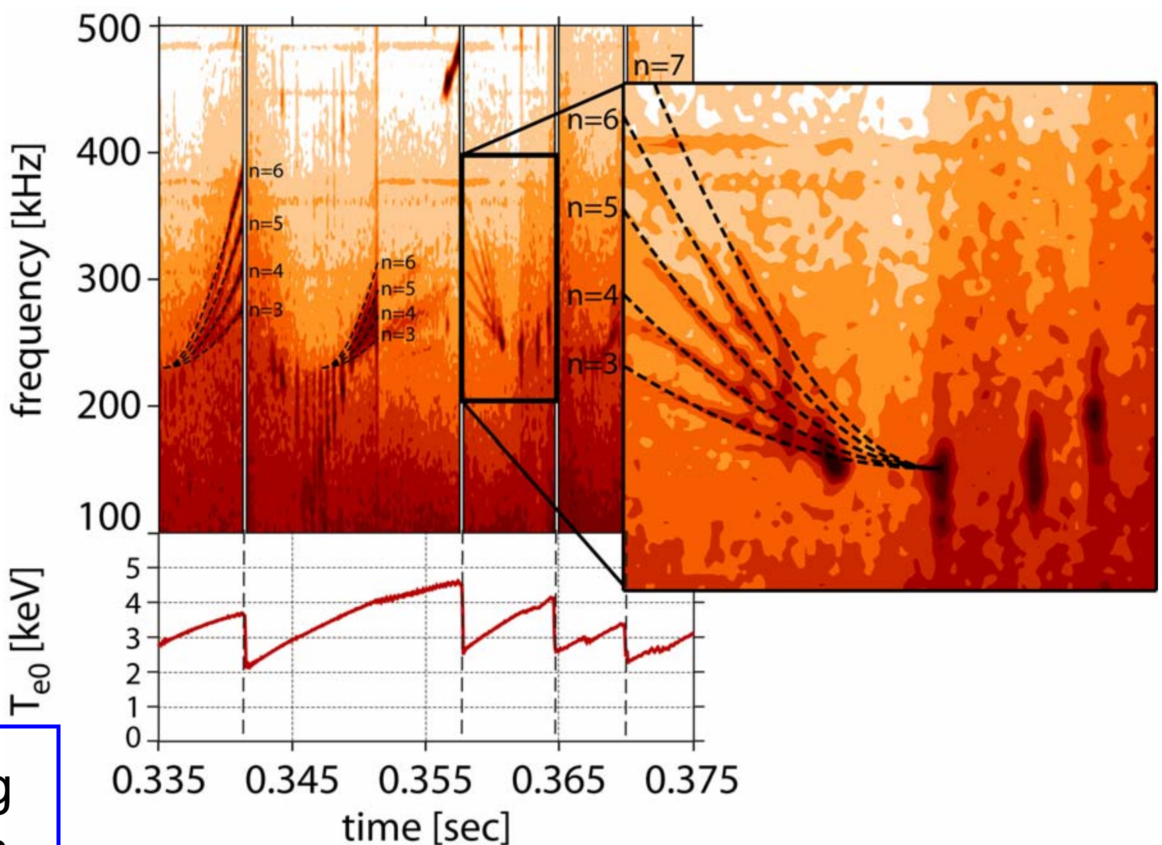

Down-chirping RSAEs imply a local maximum in the q profile following the sawtooth crash

(2 clicks)

- NOVA-K finds regular RSAE solutions with q < 1 (pre-reconnection)

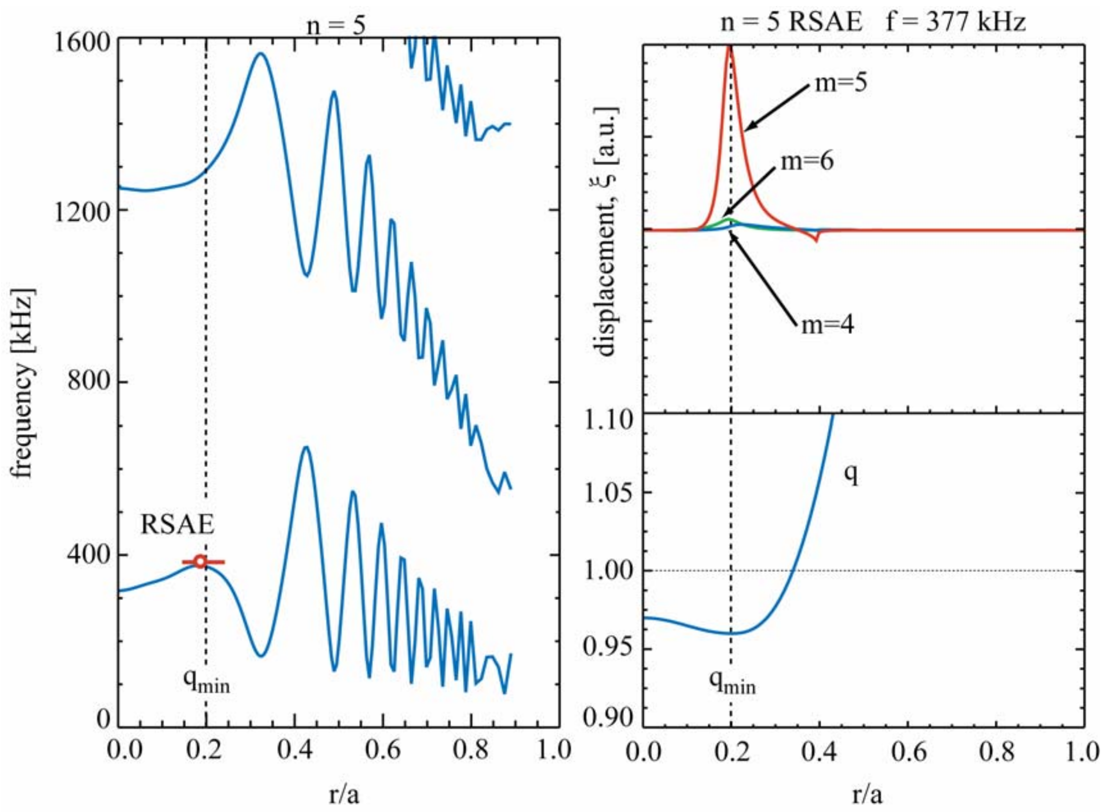

Down-chirping RSAEs imply a local maximum in the q profile following the sawtooth crash

- NOVA-K finds regular RSAE solutions with q < 1 (pre-reconnection)
- No solutions exist for a conventional reversed shear q profile with $q_{min} > 1$

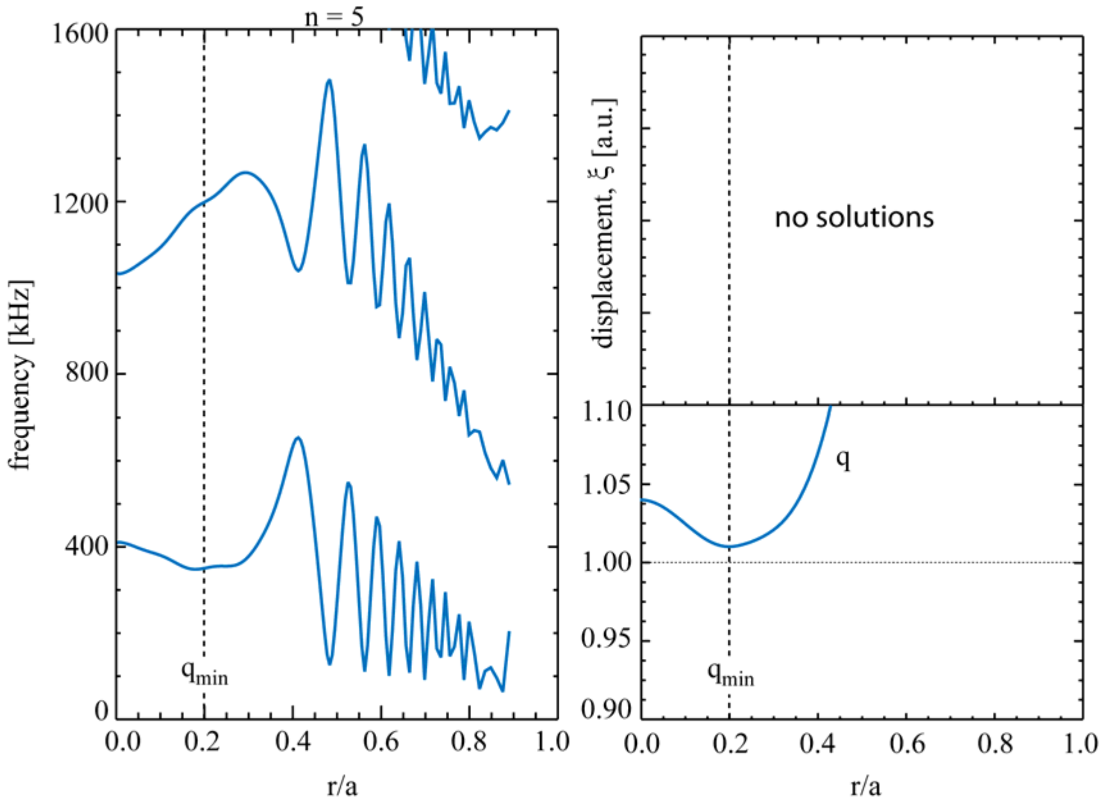

Down-chirping RSAEs imply a local maximum in the q profile following the sawtooth crash

- NOVA-K finds regular RSAE solutions with q < 1 (pre-reconnection)
- No solutions exist for a conventional reversed shear q profile with $q_{min} > 1$
- RSAE solutions do exist when the q profile has a local maximum

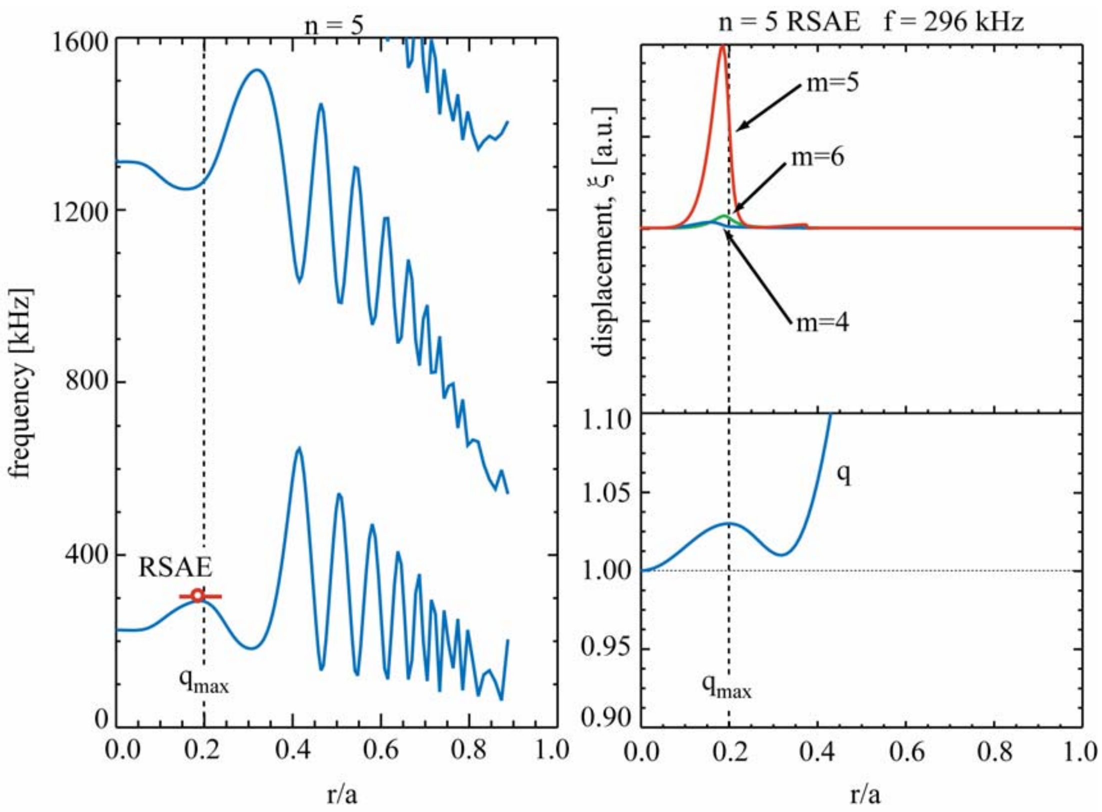

Down-chirping RSAEs imply a local maximum in the q profile following the sawtooth crash

$q_{min} < 1$

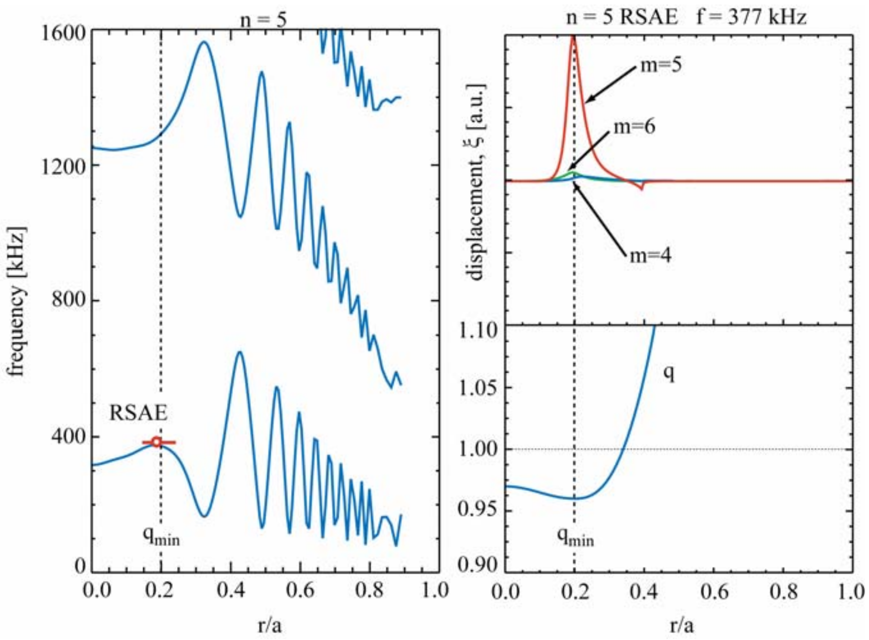

$q_{min} > 1$

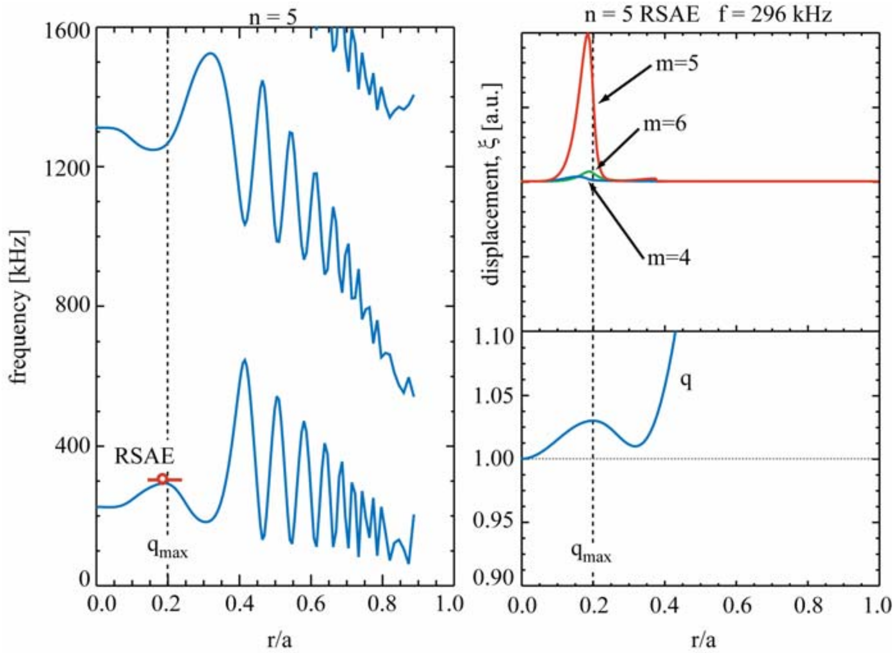

Observation of RSAEs constrains the evolution of the q profile during sawteeth

- Post-reconnection q profile has a local maximum
  - down-chirping RSAEs
- Pre-reconnection q profile has reversed shear in the region r/a < 0.2
  - up-chirping RSAEs
- A model of the sawtooth cycle requires a relaxation process and reconnection process that closes the cycle.

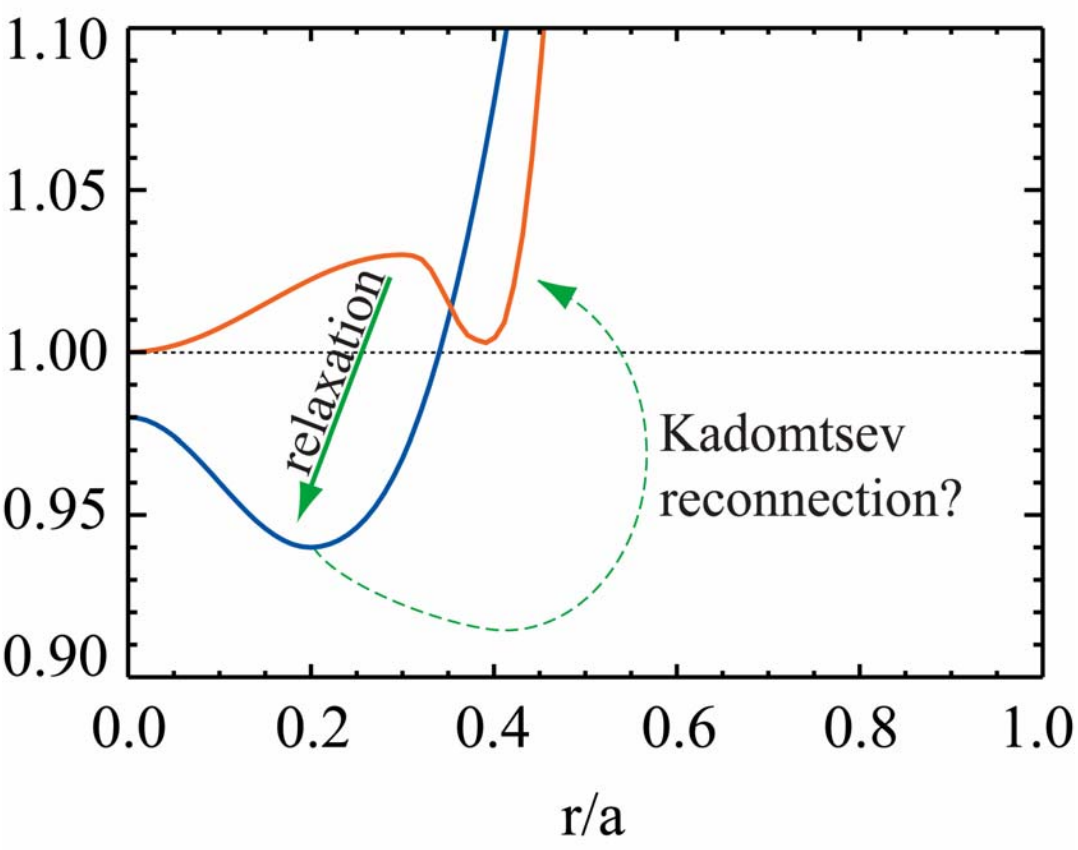

Summary

- **RSAEs observed during the current ramp phase**
  - Relatively quiescent window for the study of the interplay between RSAEs and energetic ions
  - The coupling of core modes to the magnetics needs more work
    - Experiments underway, more modeling needed
  - Minimum frequency bounds the adiabatic index to $1.25 \leq \gamma \leq 1.55$
    - Are energetic ion contributions important?
    - How to model the plasma compressibility in the limit $k_{||} \rightarrow 0$?
    - Can an effective adiabatic index be derived from simulation?

- **RSAEs frequently observed during sawteeth with $n_{e0} < 1.5\ 10^{20}\ m^{-3}$**
  - Experiments at C-Mod conducted in ITER relevant conditions
  - RSAEs offer the possibility of core MHD spectroscopy during sawteeth
  - Down-chirping RSAEs suggest a local maximum
  - Kadomtsev model could possibly explain the observed RSAEs

Alcator C-Mod

Evidence of non-linear RSAE harmonics

Harmonic frequency range

Fundamental frequency range

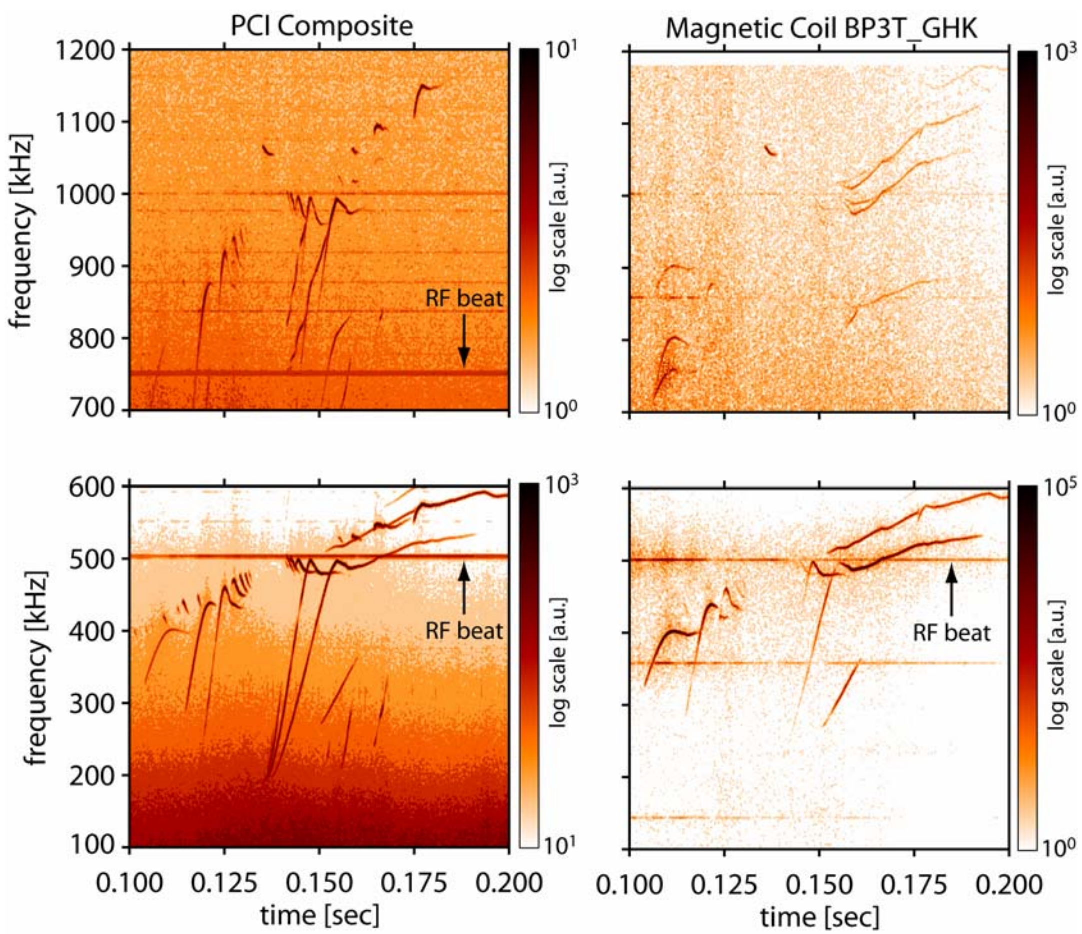

2nd order perturbations represent mode coupling of like and unlike toroidal mode numbers

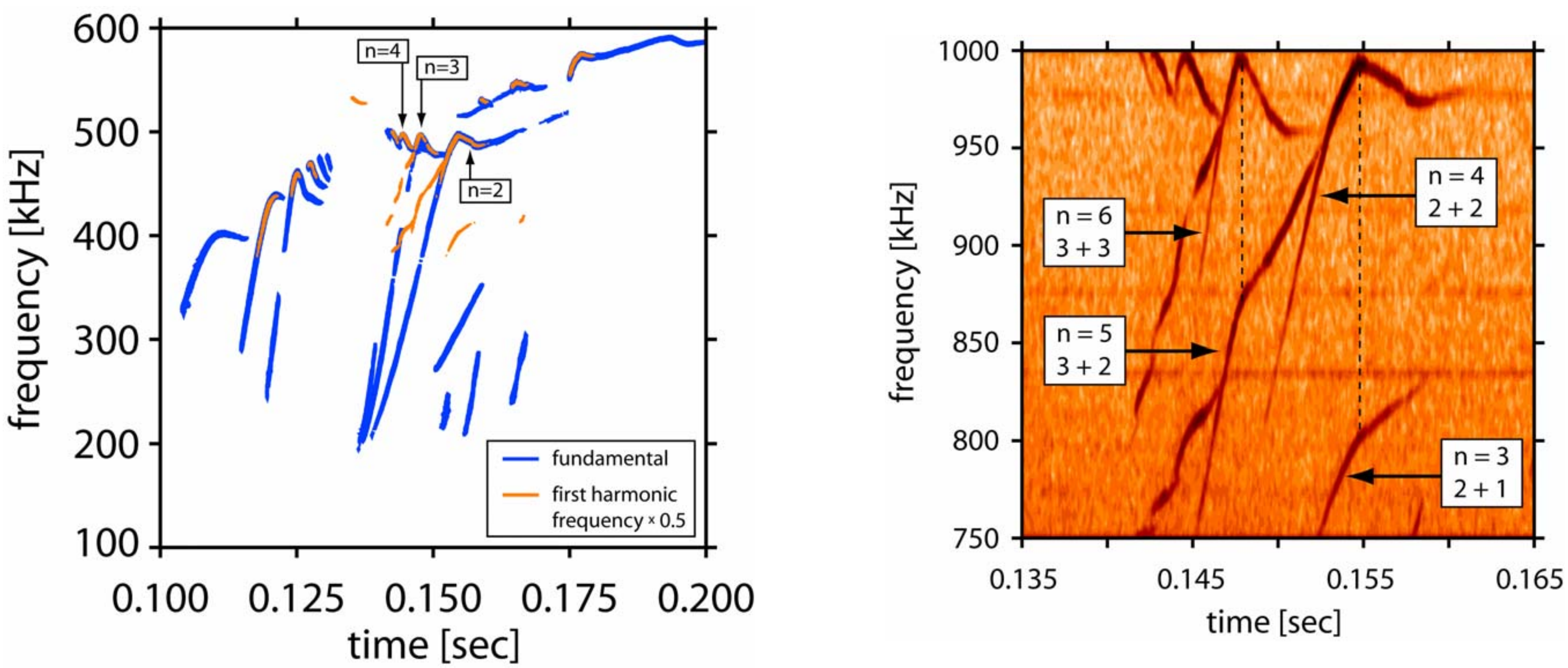

Phase contrast imaging transforms phase variations to intensity variations

Without phase plate

$$I_{PCI} \sim E_0^2 \left|1 + i\Delta\right|^2 \sim E_0^2 (1 + \Delta^2)$$

With phase plate

$$I_{PCI} \sim E_0^2 \left|i + i\Delta\right|^2 \sim E_0^2 (1 + 2\Delta)$$

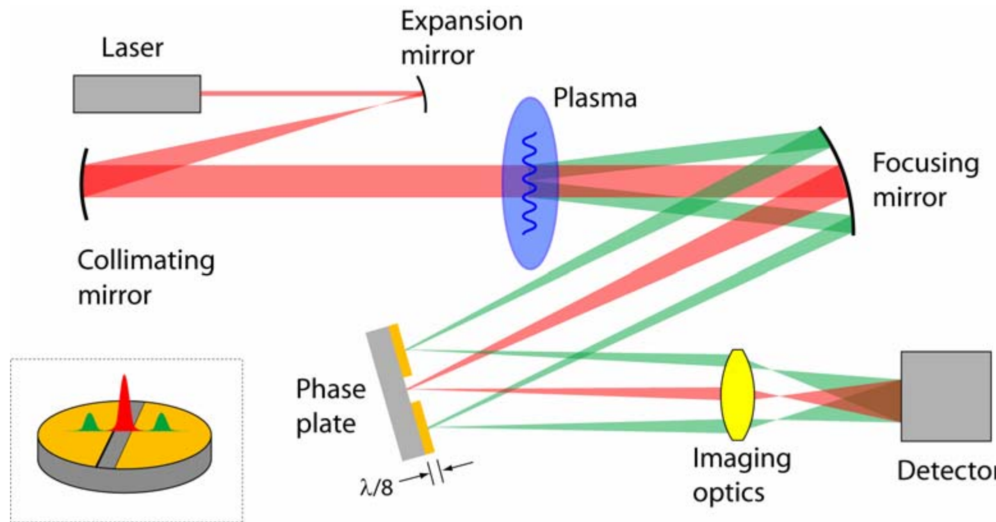

$$\Delta(x) = \frac{\omega_0}{c} \int \widetilde{N}(x, z)\, \mathrm{dz}$$

$$= \underbrace{\left(\frac{e^2}{4\pi\varepsilon_0 m_e c^2}\right)}_{r_e} \lambda_0 \int \widetilde{n}_e(\mathrm{x}, \mathrm{z})\, \mathrm{dz}$$

$$\boxed{\Delta(x) = r_e \lambda_0 \int \widetilde{n}_e(x, z)\, \mathrm{dz}}$$

The Kadomtsev model can produce a local maximum in q

(2 clicks)

- Start with Kadomtsev Model[1] for reconnection
- Surfaces of equal helical magnetic flux reconnect
- Toroidal magnetic flux is conserved

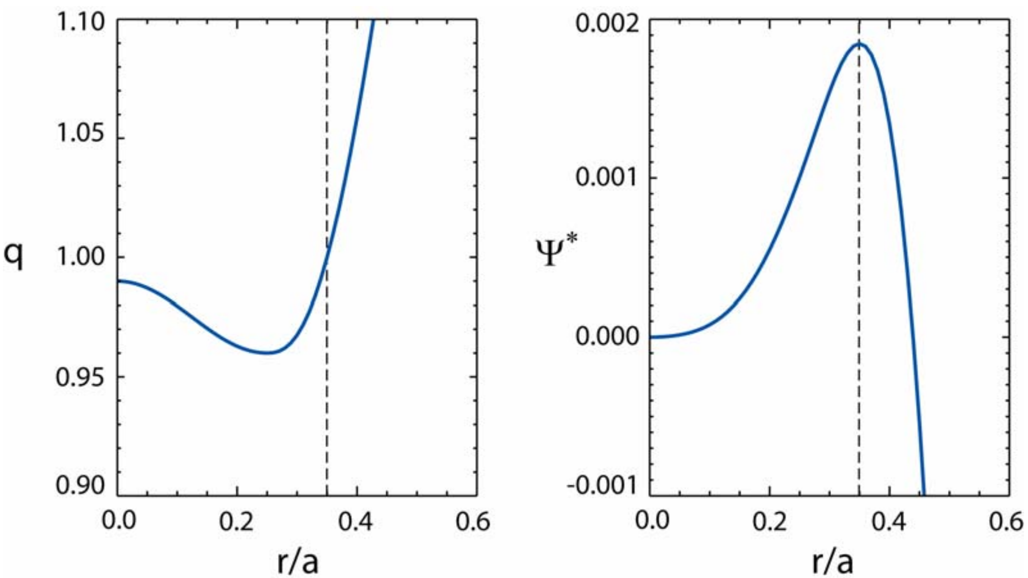

$$q(r) = \frac{1}{1 + \frac{1}{2\pi r}\frac{d}{dr}\Psi^*}$$ safety factor

$$\Psi^* = \int_0^r \left(\frac{1}{q(r')} - 1 \right) 2\pi r' dr'$$ helical magnetic flux

[1] B.B. Kadomtsev, Soviet Journal of Plasma Physics **1**, 389 (1975).

The Kadomtsev model can produce a local maximum in q

- Start with Kadomtsev Model[1] for reconnection
- Surfaces of equal helical magnetic flux reconnect
- Toroidal magnetic flux is conserved

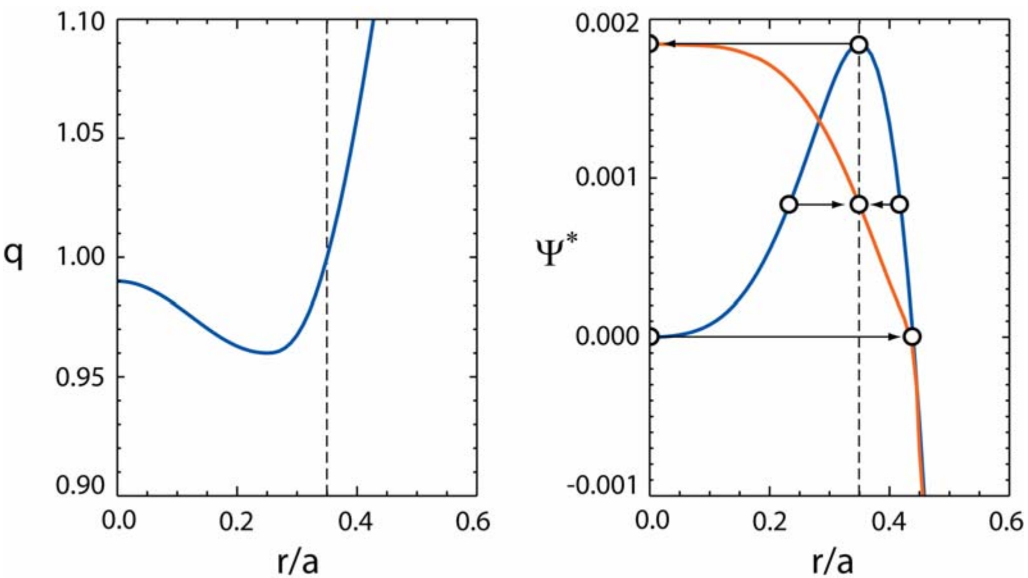

$$q(r) = \frac{1}{1 + \frac{1}{2\pi r}\frac{d}{dr}\Psi^*}$$

safety factor

$$\Psi^* = \int_0^r \left(\frac{1}{q(r')} - 1 \right) 2\pi r' dr'$$

helical magnetic flux

[1] B.B. Kadomtsev, Soviet Journal of Plasma Physics **1**, 389 (1975).

The Kadomtsev model can produce a local maximum in q

- Start with Kadomtsev Model[1] for reconnection
- Surfaces of equal helical magnetic flux reconnect
- Toroidal magnetic flux is conserved

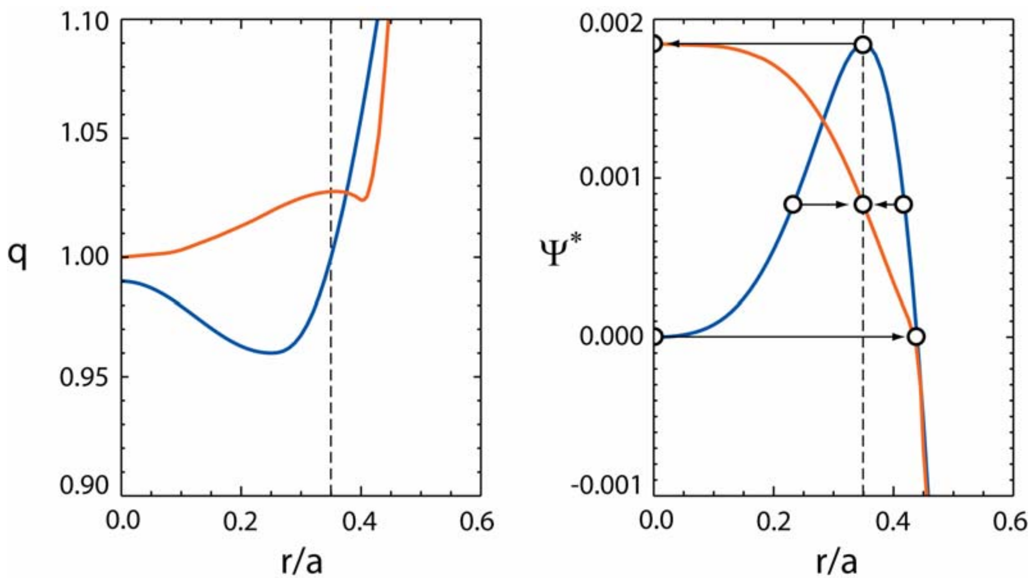

- A local maximum in q can be produced when the reconnection starts from a reversed shear q profile

$$q(r) = \frac{1}{1 + \frac{1}{2\pi r}\frac{d}{dr}\Psi^*}$$

safety factor

$$\Psi^* = \int_0^r \left(\frac{1}{q(r')} - 1\right) 2\pi r' dr'$$

helical magnetic flux

[1] B.B. Kadomtsev, Soviet Journal of Plasma Physics **1**, 389 (1975).